Tunnel investigations of metals at high pressures

V. M. Svistunov, M. A. Belogolovskiĭ, and O. I. Chernyak

Physicotechnical Institute, Academy of Sciences of the Ukrainian SSR, Donetsk

Usp. Fiz. Nauk **151**, 31–66 (January 1987)

A review is given of the results obtained by the method of tunnel spectroscopy in high-pressure studies of superconductivity, lattice properties, size quantization effects, and Andreev reflection. Experimental data on changes in the superconducting energy gap, its anisotropy, phonon spectra, and spectral electron-phonon interaction function are reported and analyzed. The limits of validity of approximate formulas for the critical temperature of a superconductor are discussed. Investigations are reported of the behavior of the electron phonon interaction and of vibrational spectra of the lattices of binary systems near the phase equilibrium boundaries. Studies of the influence of pressure on the quantum size effect in thin metal films and of interference effects in superconductor-normal metal layer structures are used to find the shift of the high-energy characteristics of the band structure and an increase in the Fermi velocity is reported. Potential applications of the method of electron tunneling in the physics of high pressures are discussed.

CONTENTS

1. INTRODUCTION

It is difficult to overestimate the role played by high pressures in modern physics: it is the basis of advanced technology for the processing of materials and preparation of new substances with unusual properties. The technique of high pressures is used widely in experimental physics. This has been largely due to the progress made in developing methods for creation of static pressures of 10^4–10^6 bar and for building the necessary apparatus in the form of high-pressure chambers now available in many laboratories.

However, some experimental difficulties in determination of the various properties of matter at high pressures still remain. This applies particularly to investigations of the energy spectra of quasiparticles, representing one of the central problems in solid-state physics. This is because the traditional methods for the investigation of the energy spectra of conduction electrons (cyclotron resonance, ultrasound, etc.) and of the vibrational spectrum of the lattice (inelastic neutron scattering, specific heat measurements) are either impossible to use or require solution of difficult technical problems when these methods are combined with high pressures, low temperatures, and strong magnetic fields.

These situations have stimulated the search for and the development of new investigation methods. The tunnel spectroscopy method is very attractive from this point of view.[1–3] The energy range accessible to this method extends above the Fermi energy and well above the Debye energy, and is limited only by the height of the potential barrier (amounting to a few electron volts). Tunnel experiments can provide data on the spectra of elementary excitations of the Fermi and Bose types (electrons, phonons, magnons, etc.) and on the interactions between quasiparticles determining various physical properties. From the experimental point of view an equally important circumstance is that the tunnel method is essentially resistive, so that all the physical information is provided by the current-voltage characteristic. Electrical measurements are probably the most widely used in physics of high pressures and the problem of passing electrical leads into high-pressure chambers with samples can be regarded as fully solved.

The greatest achievement of tunnel spectroscopy is a better understanding of the nature of superconductivity.[4] The proof of the energy gap in the spectrum of excitations in a superconductor[4] and manifestations of the phonon spectrum in the conductivity of superconducting tunnel con-

 0038-5670/87/010001-22$01.80

tacts[5,6] were reported already in the early sixties. A theory of superconductivity with a strong electron-phonon interaction (EPI) owes much to the tunnel effect.[7,8]

At the same time an interesting situation in relation to the effects of pressure on the superconductivity was developing. Very large amounts of data were available on the changes in macroscopic parameters T_c and H_c. However, N. B. Brandt and N. I. Ginzburg pointed out in 1969 that the available data on the mechanism of the influence of pressure on T_c were contradictory.[9] Therefore, the use of the tunnel effect in investigations of this kind was essential and one could expect basically new results.

Investigations of the influence of high pressures on electron tunneling in metals were started in 1967. Lead, a superconductor with a strong EPI, was the first material to be investigated at pressures up to 15 kbar at the Donetsk Physicotechnical Institute of the Ukrainian Academy of Sciences (Ref. 10), as well as at the Institute of Physics of Semiconductors of the USSR Academy of Sciences and the Institute of High-Pressure Physics of the USSR Academy of Sciences (Ref. 11),[1)] and at 3.5 kbar at Edmonton University, Canada (Refs. 12 and 13). Later A. A. Galkin *et al.* reported the results of measurements under pressures up to 14 kbar on the energy gap in superconductors with a weak EPI,[14,15] which were tin, indium, and thallium. These first experiments revealed that the critical temperature varied more rapidly than the energy gap and provided information on the shift of the phonon spectrum.

The research on this topic was later started at other laboratories, such as those at the State University of New York, Birmingham, N. Y. (Ref. 16), University of Paris-Sud, Orsay (Refs. 17 and 18)(, Laboratory for Electronics and Applied Physics, Limeil-Brevannes, France (Ref. 19), Institute for Nuclear Reseach, Julich, West Germany (Ref. 20); this work also stimulated theoretical investigations.[21–23]

At the Donetsk Physicotechnical Institute the method of tunnel spectroscopy was used to carry out high-pressure studies of superconductivity, lattice and electronic properties, quantum size effects, barrier properties, and phase transitions. In the course of these investigations a "dispersion" method was developed for the determination of the complex gap parameter of a superconductor and reconstruction of the spectral function of the EPI,[24–27] and a modulation method for recording tunnel characteristics was introduced.[27–29]

The task of the present review is to summarize the investigations carried out at various laboratories on the tunnel phenomena at high pressures. Attention will be concentrated on the physics of these phenomena. An important result of this work is the availability of data on changes in the energy gap of superconductors, phonon spectra, and spectral function of the EPI under pressure. This is basically new information. Together with the results of studies of the tunnel size effects, it has made it possible to solve the problem of the mechanisms responsible for the changes in the critical temperature of superconducting nontransition metals.

2. MAIN IDEAS ON THE TUNNEL EFFECT IN METAL-INSULATOR-METAL STRUCTURES

The phenomenon of passage of microparticles through high potential barriers has been known from the foundation of quantum mechanics as the tunnel effect. The problem of the tunnel currents in solids has been discussed theoretically right from the beginning. However, extensive studies of tunnel processes started in the sixties when a technology for the preparation of tunnel contacts has been developed and attractive practical applications of the tunnel phenomena have been suggested.[1,30]

The traditional object of these investigations is a metal-insulator-metal (MIM) layer structure. The progress has largely depended on the skill of the experimenter who had to be capable of fabricating a barrier in the form of a very thin homogeneous insulator layer ($\sim 10^{-7}$ cm) to ensure flow of a tunnel current between the metals. The "classical" variant of a metal-vacuum-metal structure was realized only in the eighties and this has made it possible for the construction of a high-resolution tunnel scanning microscope.[31]

In the case of an MIM contact the height and shape of the potential barrier $\varphi(z)$ (z is the direction along the normal to the electrode surface) are governed by the work functions of electrons in the metals. Usually the metal-insulator interface is regarded as a flat plane[2)] and $\varphi(z)$ is approximated by a trapezoid on the assumption that

$$\varphi(z) = \bar{\varphi} + \left(\frac{z}{d} - \frac{1}{2}\right)\Delta\varphi, \tag{2.1}$$

where $\bar{\varphi}$ and d are the average height and thickness of the barrier and $\Delta\varphi = \varphi(d) - \varphi(0)$. The current-voltage characteristic $I(U)$ of a tunnel structure then depends on the parameters $\bar{\varphi}$, d, and $\Delta\varphi$. In particular, at low values of $U \ll \bar{\varphi}$ the differential conductivity $\sigma(U) = dI/dU$ is a parabola, the center of which is shifted along the voltage axis relative to $U = 0$ by an amount[33]

$$U_{\min} = \frac{0{,}65\Delta\varphi}{d\bar{\varphi}^{1/2}}. \tag{2.2}$$

Investigations of the elastic component of the tunnel current in an MIM system can provide data on the quasiparticle spectra of metals serving as the electrodes of the contact[2,3] and studies of the inelastic component can provide information on the molecular spectra of impurities in the insulator, as well as on the vibrational spectra of the barrier and the barrier region near the electrodes.[34] A consistent derivation of an expression for the current-voltage characteristic of an MIM structure shows that the elastic component of the tunnel current is governed by the spectra intensities of electron excitations in metals $A(\mathbf{k},\omega)$ (Ref. 35):

$$J(U) = \frac{4\pi e}{\hbar}\sum_{\mathbf{pq}} |T_{\mathbf{pq}}|^2 \int d\omega A^{(1)}(\mathbf{q}, \omega - U) A^2(\mathbf{p}, \omega) \times [f(\omega - U) - f(\omega)], \tag{2.3}$$

where

$$f(\omega) = \left[\exp\left(\frac{\omega - \varepsilon_F}{T}\right) + 1\right]^{-1}$$

is the Fermi distribution function; the temperature T and the voltage U are measured in energy units; $T_{\mathbf{pq}}$ is a tunnel matrix element describing a transition of an electron from one contact electrode with a momentum $\mathbf{p}$ to another with a momentum $\mathbf{q}$. The function $A(\mathbf{k},\omega)$ describes the probability that an electron with a given momentum $\mathbf{k}$ has an energy ω and this function is related directly to the electron Green's function.[35]

If we substitute in Eq. (2.3) the expression for the spec-

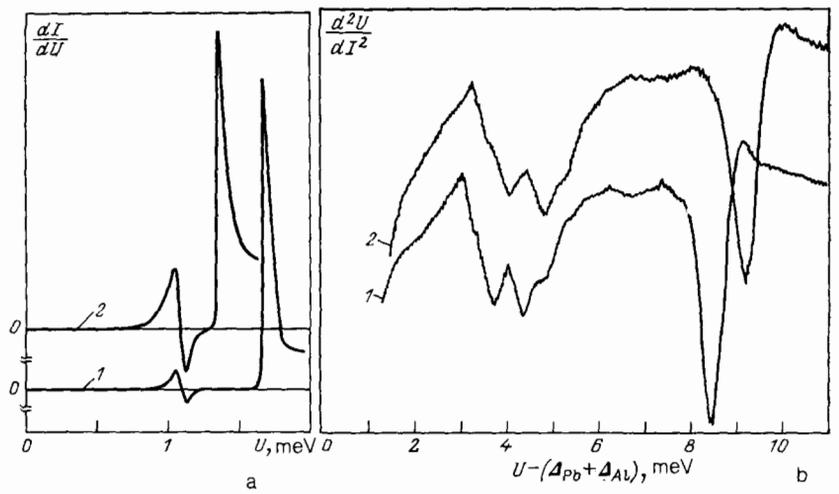

FIG. 1. Manifestations of the energy gap and of the phonon spectrum in tunnel characteristics of an Al-I-Pb contact in the superconducting state[53]: a) differential conductance dI/dU plotted as a function of U; b) second derivative of the current-voltage characteristic d^2U/dI^2 plotted as a function of U. Measurements at a temperature $T = 1.17$ K and pressures: 1) $P = 0$; 2) 12.2 kbar.

tral function $A(\mathbf{k},\omega)$ valid for normal (N) metals and assume that $|T_{pq}|^2 = \text{const}$, we find that the current-voltage characteristic $I(U)$ is linear: $I_{NN}(U) = \sigma_0 U$, i.e., $\sigma_{NN}(U) = \sigma_0 = \text{const}$. In the case of NIS contacts, when one of the electrodes is superconducting (S), similar transformations yield the following expression for the differential conductivity $\sigma_{NS}(U)$ (Ref. 35):

$$\sigma_{NS}(U) = \sigma_0 \operatorname{Re} \frac{U}{(U^2 - \Delta^2(U))^{1/2}}, \qquad (2.4)$$

where $\Delta(\omega)$ is the complex parameter of the energy gap satisfying the relationship $\Delta(\Delta_0) = \Delta_0$; Δ_0 is the gap in the energy spectrum of the superconductor. The square root singularity of $\sigma_{NS}(U)$ which appears in the limit $U \to \Delta_0 + 0^+$ makes it possible to find experimentally the energy gap of the superconductor. If another superconducting metal with a gap Δ_1 is used as the injection source, then the differential conductivity of an S_1IS structure has two singularities at energies $\Delta_0 \pm \Delta_1$ (Ref. 6), which makes it possible to find simultaneously both Δ_1 and Δ_0 (Fig. 1a).

According to Eq. (2.4), the $\sigma_{NS}(U)$ and $\sigma_{SS}(U)$ curves reflect the form of the complex dependence $\Delta(\omega)$, which in turn is related by nonlinear integral Eliashberg equations[36] to the electron-phonon interaction function $g(\omega)$. Consequently, tunnel experiments on superconductors make it possible to determine directly the critical points in the density of the phonon states. Scalapino and Anderson[37] demonstrated that these critical points are manifested by singularities of the fine structure of the second derivative d^2U/dI^2 (Fig. 1b). It is thus possible to obtain information on the phonon spectrum of a metal and on the influence of external factors on this spectrum.

The tunnel experiments represent effectively one of the variants of the solution of the important problem of calculating superconducting properties. They make it possible to reconstruct the EPI function $g(\omega) = \alpha^2(\omega)F(\omega)$ describing the superconducting state [$F(\omega)$ is the phonon density of states]. According to Eq. (2.4), a determination of the differential conductivity of an NIS contact in the superconducting and normal states can give the tunnel density of states

$$N_t(\omega) = \operatorname{Re} \frac{\omega}{(\omega^2 - \Delta^2(\omega))^{1/2}}. \qquad (2.5)$$

The subsequent procedure in the analysis of the tunnel characteristics involves the use of a dispersion relationship[24] relating the real and imaginary parts of the complex function:

$$\operatorname{Im} \frac{\omega}{(\omega^2 - \Delta^2(\omega))^{1/2}} = \frac{2\omega}{\pi} \int_{\Delta_0}^{\infty} \frac{N_t(\omega') - N_{BCS}(\omega')}{\omega^2 - \omega'^2} d\omega'. \qquad (2.6)$$

Here and later we are assuming that $\omega \geqslant 0$; $N_{BCS}(\omega) = \operatorname{Re}[\omega/(\omega^2 - \Delta_0^2)^{1/2}]$ is the tunnel density of states in the Bardeen-Cooper-Schrieffer (BCS) theory. The relationship (2.6) follows from general analytic properties of the Green's functions[25] and it does not require solution of the Eliashberg equations. This makes it possible to find $\Delta(\omega)$ for any pairing mechanism. The function $\Delta(\omega)$ calculated in this way is essentially a new (additional to the critical parameters T_c, H_c, and the gap Δ_0) experimental characteristic of a superconductor. When the function $\Delta(\omega)$ is known, the nonlinear Eliashberg equations reduce to an integral equation which is linear in terms of $g(\omega)$ (Ref. 25). This equation can be solved using a computer of moderate power, of the kind that is usually available to experimental research groups. The final stage of the analysis of the tunnel data for superconductors involves calculation of the various characteristics of these materials and a comparison with the measured values. The critical temperature T_c calculated from the exact relationships using the functions $g(\omega)$ is of fundamental importance to the method of checking experimental and theoretical results. The detailed program for calculating the EPI function of a superconductor on a computer was reported in Ref. 26.

In the case of transitions metals, i.e., metals of elements with partly filled d shells, as well as their alloys and compounds, the procedure of reconstruction of the function $g(\omega)$ from the tunnel data has a number of special features. This is because the potential barriers formed by transition metal oxides are frequently low, so that it is important to allow for the dependence of the barrier transparency on the bias voltage. This modifies the relationship between the tunnel density of states and the measured characteristics[38]:

$$N_t(U) = \frac{\sigma_{NS}(U)}{\sigma_{NN}(U)} \mp \frac{\beta\Delta_0^2}{(U^2 - \Delta_0^2)^{1/2}}, \qquad (2.7)$$

where $|U| > \Delta_0$ and the sign in Eq. (2.7) is identical with the polarity of the potential applied to the investigated super-

conductor, whereas the coefficient β is found from the condition of minimum discrepancy between the calculated and corrected density of states.[28]

Another important circumstance is that in the majority of transition metals the mean free path of an electron excitation with a typical phonon energy is ~ 100 Å or even less. Consequently, even a slight contamination or imperfection of the structure of a metal surface adjoining an insulator has a major influence on the results of tunnel measurements.[39] In such a case it is desirable to investigate NIS(S) contacts with a very thin (tens of angstroms) layer of the normal metal separating the transition metal superconductor from the insulator. An allowance for the proximity effect modifies the "dispersion" method of reconstructing the function $g(\omega)$ of a superconductor. A solution of this problem within the framework of the tunnel model of the proximity effect[40] is given in Ref. 41. The approach utilizing the interference model[42] is described in a review given in Ref. 43.

We have pointed out that the range of applications of the "dispersion" method is not limited to finding the EPI function of a superconductor from the experimental data. It can be used in specific calculations of the properties of superconducting materials.[44–46] and in the reconstruction of the properties of a normal metal from the self-energy corrections to the differential conductivity of NIN contacts.[3,27,134]

There is also another iteration procedure of solving the Eliashberg equations in reconstruction of the EPI function of a superconductor.[47]

3. EXPERIMENTAL METHODS

It is difficult to imagine the development of research on the tunnel effect in solids without the ingenious solution of the barrier problem by Giaever.[5] It is due to Giaever that the vacuum method of condensation of metals has become the main technology of preparation of tunnel contacts. The equipment required for this technology is not particularly complex. Vacuum of 10^{-5}–10^{-6} Torr is readily attainable and quite sufficient for the preparation of the objects to be investigated. A barrier is formed by oxidation of the first film before the deposition of the second. Air or oxygen in controlled amounts is a good oxidizing medium for the creation of barriers of different thicknesses and with different resistances. Substrates are usually standard glass cover plates. In the final form a tunnel sample of the metal-oxide-metal type is cross-shaped: the intersection between two films forms the actual tunnel contact and the other parts of the films act as current and potential terminals for connection to the measuring circuit.

This type of sample has been used in the majority of the investigations discussed below. Aluminum is used as the injector and its oxide has sufficient mechanical strength throughout the investigated range of pressures. The precision and resolution of the structure of the tunnel characteristics can be improved using superconductor-oxide-superconductor (S_1IS) contacts, and is done by the experimental groups in Donetsk, Moscow, and West Germany, or by using NIS contacts, as is done in all the other laboratories.[31] It should be pointed out that the main difficulty in the Giaever technology is the preparation of a thin oxide film which has the same thickness over the whole contact area. Introduction of the high pressure techniques has made the requirements in respect of the tunnel contacts much more stringent, since weak points can appear in the barrier and these can lead to metal short-circuiting paths and even to damage. In our laboratory we were able to master the preparation of aluminum oxides so that in 7–8 cases out of 10 we can avoid the contribution of the leakage currents of nontunnel nature when contacts are compressed at pressures up to 18 kbar at temperatures down to 1 K in magnetic fields up to 30 kOe and thermal cycling involves variation of the temperature of a sample from room to liquid nitrogen and liquid helium and back again. High-quality barriers capable of withstanding high pressures have also been prepared by oxidation of bulk niobium and tantalum.[38] Lead and tin oxides, which are used in studies of the Josephson effects, are unsuitable for studies under pressure.

Promising results have been reported for Schottky barriers[17–19]: data have been reported for oxide contacts with lead and indium and a superconducting modification of bismuth has been studied at 30 kbar. In these investigations lead, indium, and bismuth were deposited in vacuum down to 10^{-10} Torr on carefully prepared n-type GaAs single-crystal surfaces. Such tunnel contacts are less senstive to inhomogeneities of mechanical pressures and they can therefore be used at much higher pressures than those considered below.

Hydrostatic compression of tunnel contacts is ensured by the pressure "freezing" method.[9,48] in the laboratories of the Institute of Semiconductor Physics and the Donetsk Physicotechnical Institute use is made of a chamber with a kerosene-oil mixture developed at the Institute of High Pressures.[49] At helium temperatures it is possible to reach reliably pressures of about 15 kbar in this chamber. In some experiments carried out at the Donetsk Physicotechnical Institute use has been made also of the ice technique proposed at the Kharkov Physicotechnical Institute of the Ukrainian Academy of Sciences.[50]

In studies carried out at Edmonton University and at the State University of New York on lead and lead-indium alloys use was made of solid helium to produce pressures up to 3.5 kbar.[12,13,16] At the Institute for Nuclear Research in Julich studies have been made of lanthanum at 17.5 kbar using a mixture of n-pentane with isoamyl alcohol.[20] Isopentane has been employed in a study of Schottky barriers (GaAs/Pb, GaAs/In)[18,19] under a pressure of 17 kbar; pressures of 30 kbar have been applied to Bi III in a bomb containing a mixture of isoamyl alcohol and isopentane.[17]

Investigations at the Donetsk Physicotechnical Institute have shown that the most convenient and reliable method of connection to a measuring circuit is provided by a shutter construction with sealing of the leads in accordance with the unsupported area principle.[51–53] This makes it possible to introduce 24–26 conductors into a chamber (bomb) with a working channel 6 mm in diameter. It is thus possible to study simultaneously 6–8 tunnel contacts on 2–3 substrates under pressure, to carry out resitive measurements of the critical temperature of the films forming the contacts, and to use tin and indium wires as pressure sensors. The samples and pressure sensors are placed at the center of the bomb channel, which minimizes the influence of possible departures from hydrostatic compression conditions. The error in the determination of the pressure in the bomb does not exceed 2%. The bomb with the samples is placed directly in

liquid helium. Reliable monitoring of the shifts of the tunnel spectra outside the bomb is provided by contacts prepared in the same cycle as those placed in the high-pressure chamber.

Low temperatures down to 1.17 K are reached by pumping out helium vapor from a cryostat with liquid nitrogen and helium screens. The cryostat is fitted with a superconducting solenoid which can create magnetic fields of about 20 kOe. The critical temperature of the contact films can be determined by the usual resistive method and by the tunnel effect method. The latter provides an opportunity for local probing of the gap and of the value of T_c (Ref. 54) directly in the tunnel contact region ($\lesssim 0.5$ mm^2). This avoids broadening of the superconducting transition due to inhomogeneity of the film along its length. The error in the measurements is ± 0.005, i.e., the critical temperature and the energy gap are in fact determined for each sample. This is particularly important because the scatter of T_c of the films (particularly those of tin, indium, and their alloys) may reach 1% or more, depending on the preparation conditions.

All the necessary physical information on the investigated sample is provided by the current-voltage characteristic and its derivatives. The dependences of he differential conductance dI/dU on U and the dependences of d^2I/dU^2 on U are determined by the well-known modulation method. It is based on the detection of harmonics which are generated by a nonlinear component on application of a harmonic signal at a frequency f. The voltage sources are effectively operational amplifiers.[55–57]

Paoli and Svacek[58] proposed a two-frequency modulation for the determination of the second and higher order derivatives. This method is based on modulation at two different but synchronous frequencies f_1 and f_2 in order to generate a signal of the derivative at the combination frequency, which corresponds uniquely to the selected order of the derivative. A suitable choice of these frequencies makes it possible to relax considerably the requirements in respect of the frequency selectivity of the electronic circuits compared with the case of harmonic selection. Moreover, this approach eliminates signals due to nonlinear distortions of the modulating signal, because the combination frequency at which the derivative signal is recorded differs from the harmonics of the modulation frequencies.

The methods discussed above are based on the assumption that the amplitude of the modulating signal is small. It is proposed in Ref. 28 that this amplitude should be increased. An algorithm for the calculation of the derivatives of the current-voltage characteristic of the investigated nonlinear structure from the amplitudes of the harmonic components was developed for this purpose.[29] This led to the construction of a tunnel spectrometer representing a combination of measuring and computing apparatus.[27] The use of a minicomputer in tunnel experiments was mentioned also in Refs. 59 and 60.

4. BARRIER PROPERTIES OF TUNNEL CONTACTS

In the calculation of the current-voltage characteristic $I(U)$ of a tunnel contact over a wide range of voltages, considerably greater than the phonon energies, we can ignore the structure of the function $A(\mathbf{k},\omega)$ due to the EPI and confine ourselves to the energy dependence of the tunnel

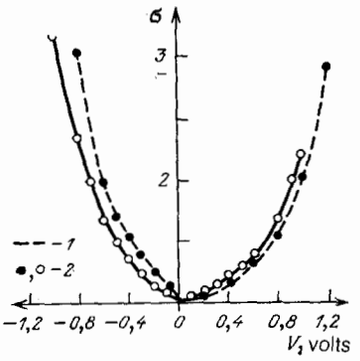

FIG. 2. Change in the "barrier" characteristic under a pressure of 12.2 kbar (continuous curve).[53] Al–I–Pb contact: 1) $P = 0$; 2) experimental points. $T = 4.2$ K, $H = 5$ kOe.

matrix element T_{pq} [see Eq. (2.4)]. The approximations used for this purpose are frequently based on the hypothesis of a vacuum gap with a trapezoidal shape of the barrier given by Eq. (2.1). This approach accounts for the experimentally observed shift of the center of the $\sigma(U)$ parabola along the voltage axis relative to $U = 0$ [Eq. (2.2)]. However, it fails to account for the large (in excess of 200 meV) shifts observed, for example, in the case of aluminum-aluminum oxide-lead contacts[52] because this gives rise to changes in the barrier height $\Delta\varphi$ of the order of $\overline{\varphi}$.

The last hypothesis was contradicted by an experimental study[61] of the influence of high pressures up to 15 kbar on the tunnel characteristics of Al–I–Pb contacts in which the variable parameter was the thickness of the insulator layer. The results obtained demonstated a strong sensitivty of the asymmetry of the differential conductivity $\sigma(U)$ to the applied hydrostatic compression (Fig. 2). For example, under pressure the value of U_{min} changed from 230 meV for $P = 0$ to 110 MeV for $P = 12.2$ kbar, so that the rate of shift of the vertex of the parabola with pressure was $d(\ln U_{min})/dP = -(4.1\text{–}4.5)\times 10^{-5}$ bar^{-1}. The relative change in the barrier thickness estimated using the simplest formulas for a rectangular barrier was found to be only about 3%. The experimental value of $d(\ln U_{min})/dP$ could be obtained on the basis of the results only on the assumption that $\Delta\varphi \sim \overline{\varphi}$. However, in this case we cannot explain halving of U_{min} as a result of compression, because at pressures of the order of 10 kbar used in this case the relative change in all the characteristics of a barrier should not exceed 10%.

The contradiction is removed by employing a two-band model which takes into account the presence of the valence band of the insulator layer. It is then found that the dependence $\sigma(U)$ is a parabola shifted by U_{min}, which has its largest value $U_{min} \approx \Delta\varphi/3$ when the chemical potential level is close to the middle of the band gap.[62] Such a situation does indeed occur in the case of a tunnel contact.[27]

A comparison of the experimental and calculated results makes it possible to obtain information on some characteristics of the energy band structure of a tunnel junction. For example, the two-band approximation was used in Ref. 63 to find the effective mass of an electron m^* and the band gap E_g for tin oxide: $m^* = 0.14m$, $E_g = 3.7$ eV. The same method was employed in Refs. 64 and 65 to determine the dispersion laws $\varepsilon(\mathbf{k})$ of AlN and GaSe.

5. SPECTROSCOPY OF THE ENERGY GAP AND OF THE ELECTRON-PHONON INTERACTION IN SUPERCONDUCTORS

Although investigations of the superconductivity under pressure were started in 1925, the relatively few parameters deduced from the experimental results (in fact, T_c and H_c) limited greatly a detailed analysis of the results and their comparison with theories. C. A. Swenson pointed out in the sixties that the experimental data of sufficient precision for comparison are lacking.[66]

The extensive opportunities provided by the tunnel spectroscopy method together with its high precision have esablished a new approach to the study of the influence of hydrostatic pressure on superconducting properties. Properties of particular interest are the changes in the energy gap, which is a microscopic characteristic, and the interaction of electrons with the crystal lattice, which is the main mechanism responsible for the Cooper pairing.

5.1. Energy gap

Typical results obtained in a study of the influence of pressure on the current-voltage characteristics and their derivatives with respect to the voltage are plotted for some tunnel contacts in Figs. 3–5. All the quantitative data on the behavior of the gap are listed in Table I. The main result of these direct measurements is that the gap changes with pressure much faster than does the critical temperature, $|d(\ln \Delta_0)/dP| > |d(\ln T_c/dP|$, and this is manifested most clearly in the case of superconductors characterized by a strong EPI, such as lead and its alloys with bismuth and indium.

It is known that the deviation of the ratio $2\Delta_0/T_c$ from the BCS theoretical value amounting to 3.53 describes the strength of the EPI in the investigated material and has its maximum value for such strongly coupled superconductors as lead, mercury, etc.

The tunnel experiments established for the first time that compression of a nontransition metal causes its main superconducting parameters to approach values predicted by the BCS theory. This is easily understoood if we bear in mind the approximate expression which relates $2\Delta_0/T_c$ to the real phonon spectrum of a superconductor.[67] We then

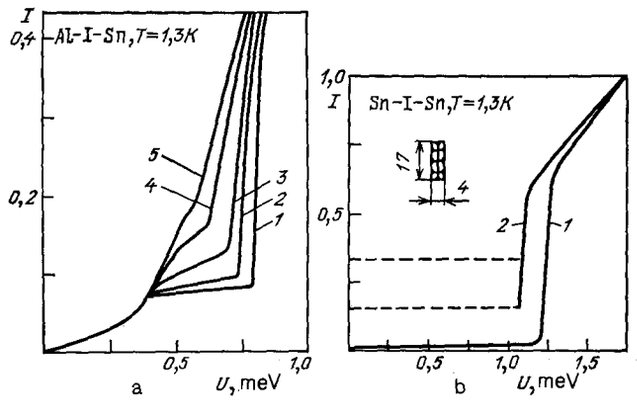

FIG. 3. Influence of pressure on the "gap" characteristics of contacts.[14] a) Al–I–Sn: 1) $P = 0$; 2) $P = 3.3$ kbar; 3) $P = 5.5$ kbar; 4) $P = 6.5$ kbar; 5) $P = 11$ kbar. b) Sn–I–Sn: 1) $P = 0$; 2) $P = 8.2$ kbar. $T = 1.3$ K.

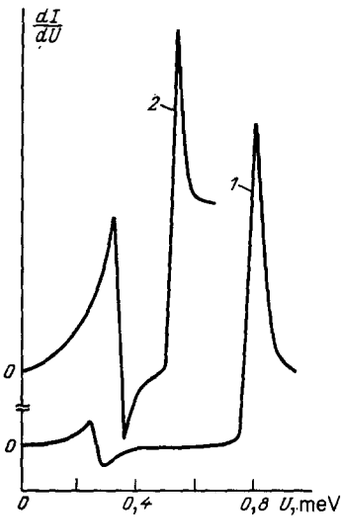

FIG. 4. Influence of pressure on the "gap" characteristics of Al–I–In contacts[15]: 1) $P = 0$; 2) $P = 14$ kbar.

have the following simple expression:

$$\frac{d \ln \Delta_0}{dP} = k \frac{d \ln T_c}{dP} - (k-1)\gamma^*, \qquad (5.1)$$

where $k > 1$, $\gamma^* = d \ln \omega_0/dP$, ω_0 is a certain average phonon frequency. It follows from Eq. (5.1) that in the case of nontransition metals with a positive value of γ^* the gap decreases faster on increase in the pressure than does the critical temperatures.[52]

These results have been obtained for films of thickness less than the coherence length ξ_0 of a superconductor. In the case of superconducting single crystals there are certain characteristic features in the tunnel conduction process due to the dependence of the gap on the crystallographic direction. The gap anisotropy effects are exhibited also by thick pure textured films in which the mean free path is considerably greater than the coherence length ξ_0 (Ref. 68). Usually the "gap" characteristics of thick lead films ($d \gtrsim 1500$ Å)

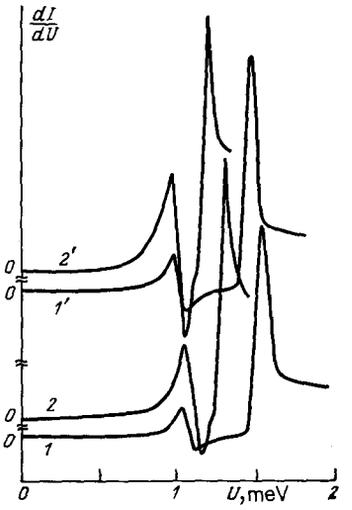

FIG. 5. Influence of pressure on the "gap" characteristics of Al–I–Bi contacts: 1), 2) Bi_2Tl; 1'), 2') ε phase; 1), 1') $P = 0$; 2), 2') $P = 12$ kbar.

TABLE I. Influence of pressure on energy gap $2\Delta_0$ and critical temperatures T_c of superconducting metals and alloys.

Material	$2\Delta_0$, meV	$\frac{d \ln \Delta_0}{dP}$, 10^{-6} bar^{-1}	T_c, K	$\frac{d \ln T_c}{dP}$, 10^{-6} bar^{-1}	P_{max}, kbar	Ref.
	2,8	−8,8±0,3	7,2	−5,3±0,3	14	53, 69, 104
Pb	2,7	−8,75±0,7	—	—	17	19
	2,71	−8	—	—	15	11
	1,24	−14,9	3,93	−12,2	11	14
Sn	1,2	−15	—	—	11	11
	1,09	−13,1±0,6	3,42	−11,1±0,5	14	15, 75
In	1,04	−14,2±0,5	—	—	11	11
	—	−11,3±0,9	—	−9,4±0,6	17	18
Tl	0,75	−3,35	2,34−2,38	−2,52	13	69
Bi III	2,7	—	7,19	—	29	17
Nb	2,08	0	9,301	−0,3	7	38
Ta	0,72	0	4,43	−0,75	9	38
La	0,8	>0	4,95	>0	17,5	20
In—Sn						
Sn, at. %:						
3	1,192	−14,5±0,6	3,64	−11,3±0,5	9,3	86
11	1,62	−9,7	4,77	−9,8	9	86
23	2,09	−12	5,88	−7,7	4	86
Pb—In						
In, at. %:						
5	2,77	−7,91±0,3	—	—	10	53, 104
	2,742	−7,05±0,54	—	—	3,6	16
12	2,72	−9,2±0,3	—	—	9,5	53, 104
	2,7	−7,63±0,48	—	—	3,6	18
	2,64	−6,16±0,3	7,11	−4,48	3,5	78
30	2,6	−8,3±0,3	6,76	−5,35	11	53, 104
36	2,48	−6,9±0,3	6,75	−4,53	3,5	78
40	2,44	−7,9±0,6	—	—	9,5	73
Pb—Bi						
Bi, at. %:						
10	3,08	−8,5±0,4	7,6	−5,2±0,4	11	105
30	3,58	−7,6±0,5	8,5	−3,2±0,5	11	105
38	3,94	−8±0,4	9	−3±0,6	10	105
Bi—Tl						
ε phase	2,36	−10,4±0,8	6,05	−7,3±0,5	12	76
Bi_2Tl	2,59	−7,1±0,7	6,61	−5,1±0,5	12	76

exhibit two gaps Δ_{min} and Δ_{max}. The extremal values of the energy gaps are $2\Delta_{min} = 2.49 \pm 0.01$ meV, 2.57 ± 0.01 meV, and $2\Delta_{max} = 2.78 \pm 0.01$ meV and 2.85 meV (Ref. 69). Similar characteristics are exhibited also by bulk samples of lead.[70] The experimental results (Fig. 6) demonstrate that the pressure-induced changes in the characteristics associated with the gap anisotropy are the same as for an isotropic gap and the rate of these changes is $-(8.6 \pm 0.6) \times 10^{-6}$ bar^{-1}.

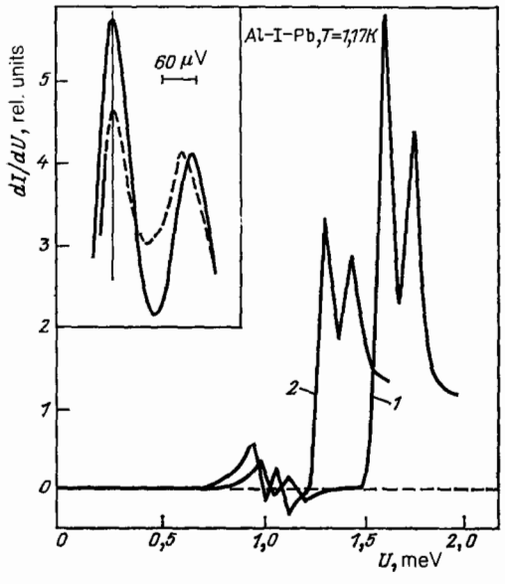

FIG. 6. Influence of pressure on the tunnel characteristics of anisotropic lead. Al–I–Pb contact[69]: 1) $P = 0$; 2) $P = 14$ kbar.

Calculations of the influence of pressure on the anisotropy of the energy gap of lead single crystals were reported in Ref. 71 together with determinations of the location of the critical points (maxima, minima, saddle points) as a function of the gap $\Delta_0(\theta,\varphi)$. The quantity A, representing the degree of anisotropy of the gap and equal to the ratio of its largest to its smallest value, increases under pressure: $A(0$ kbar$) = 1.3$, $A(20$ kbar$) = 1.19$. This is due to the fact that the parameter γ^* is assumed to be constant and, therefore, all the local values of $\Delta_0(\theta,\varphi)$ shift as a result of hydrostatic pressure at approximately the same rate. This result is in qualitative agreement with the above experimental data on the tunneling into thick textured lead films and it shows that the main factor governing the angular dependence of the parameters of lead single crystals is indeed the anisotropy of the phonon spectrum.

The anisotropy of the gap of aluminum and its changes under pressure were calculated in a similar manner in Ref. 72. However, the experimental data for this weakly coupled superconductor are not yet available.

5.2. Vibrational spectrum of the crystal lattice

Before the tunnel experiments the main source of information on changes in the vibrational spectrum of the lattice under pressure have been the direct results obtained from thermal expansion. The shift of the phonon spectrum can be

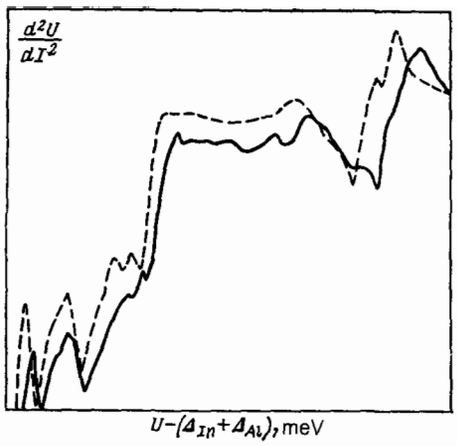

FIG. 7. Influence of pressure on the phonon structure of indium.[75] The dashed curve represents $P = 0$ and the continuous curve corresponds to $P = 10$ kbar.

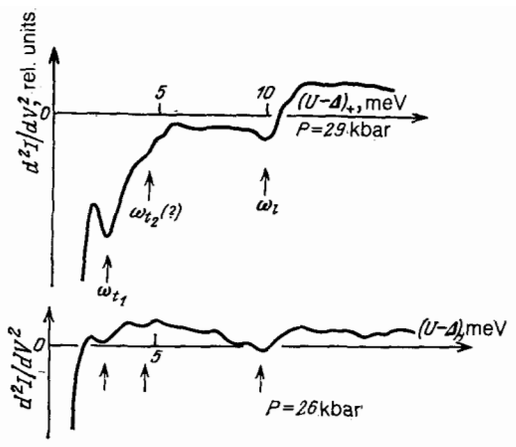

FIG. 8. Phonon structure of superconducting bismuth.[17]

estimated from the macroscopic Grüneisen parameter. The tunnel effect is now providing new opportunities to determine directly the shift of the transverse ω_t and longitudinal ω_l lattice vibrations of the investigated material and to obtain for the first time the microscopic Grüneisen parameter

$$\gamma_i(\mathbf{q}) = -\frac{d\ln\omega_i(\mathbf{q})}{d\ln\Omega} = \frac{1}{\varkappa}\gamma_i^*(\mathbf{q}),$$

where Ω is the volume, $\varkappa = -[(d\ln\Omega)/dP]_T$ is the compressibility, $\gamma_i^* = d(\ln\omega_i)/dP$ is a parameter measured in a tunnel experiment.

In our laboratory such data were obtained for lead, indium, thallium, niobium, tantalum, alloys of lead with indium, lead with bismuth, indium with tin, and bismuth with thallium.[38,53,69,73,74,75,76] Moreover, other authors investigated lead,[77] indium,[18,77] tin,[77] lanthanum,[20] bismuth,[17] and alloys of lead with indium.[16,78]

Figures 1b and 7–10 represent tunnel characteristics of some of the systems. Table II gives the experimental values of the rates of change of the phonon frequencies. A common feature of practically all the investigated elements and alloys is a linear shift of the spectrum toward higher energies [i.e., $d(\ln\omega_i)/dP > 0$]. The exceptions to this rule are:

a) lanthanum,[20] for which we have $\gamma_t^* < 0$, $\gamma_{l1}^* \approx 0$, $\gamma l\,2 > 0$ in the range of pressures up to 17.5 kbar;

b) intermetallic Bi_2Tl (Ref. 76), in the case of which the pressure of $P = 3.5$ kbar suppresses singularities of the dependence of d^2U/dI^2 on U, corresponding to the low-frequency part of the phonon spectrum (the properties of these materials will be considered later);

c) indium,[79] which exhibits at 6 kbar a nonlinear change in the singularities in the dependence of d^2U/dI^2 on U, which correspond to phonon energies.

The values of γ_i found from a tunnel experiment exceed greatly the macroscopic Grüneisen parameter γ (for example, in the case of lead we have $\gamma = 2.85$, whereas $\gamma_{t,l} \approx 3.5$) and there is a tendency for the inequality $\gamma_t > \gamma_l$ to be obeyed. This is particularly noticeable in the case of alloys. The maximum delay of the shift of the high-frequency lattice vibrations was found by us for the alloy $Pb_{0.6}In_{0.4}$ (Ref. 73) and it amounts to $\gamma_t^* \approx 2\gamma_l^*$. This effect was also observed by P. W. Wright and J. P. Franck.[78]

The results demonstrate clearly a frequency dependence of the Grüneisen parameter. They are evidence that the models based on the approximation of a constant Grüneisen parameter used to describe some properties of matter at finite pressures are too simplistic.

It is interesting to consider the behavior of the local lattice vibrations in a lead-indium alloy. The Lifshitz equation given in Ref. 80 determines their positions on the assumption that the force constants are not affected and that the perturbation of a crystal reduces to a change in the mass at one of the lattice sites. We would expect that under pres-

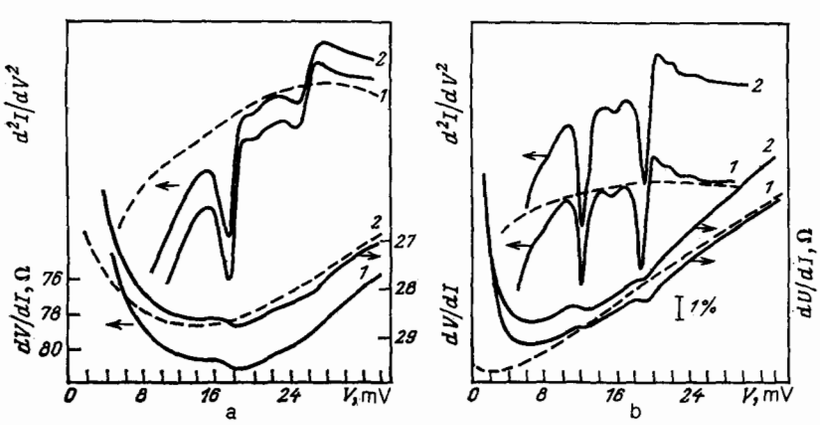

FIG. 9. Influence of pressure on the phonon structure of tantalum and niobium.[38] a) Ta–Ta_xO_y–Ag: 1) $P = 0$; 2) $P = 9$ kbar; the dashed curves represent the normal state. b) Nb–Nb_xO_y–Ag: 1) $P = 0$; 2) $P = 6$ kbar.

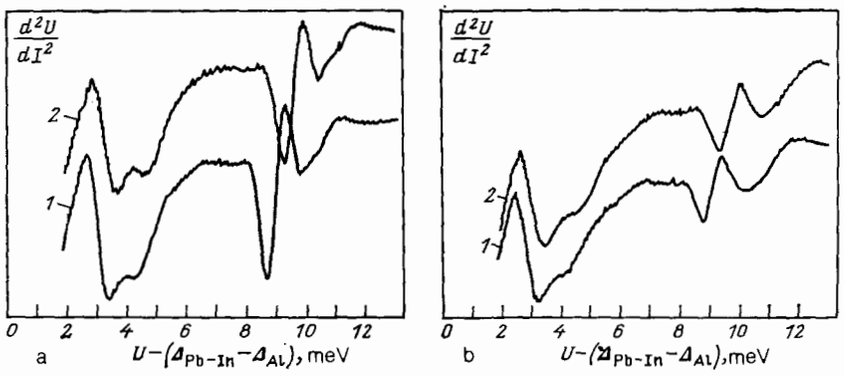

FIG. 10. Influence of pressure on the phonon structure of lead and its alloys with indium.[53] 1) $Pb_{0.08}In_{0.12}$: 1) $P=0$; 2) $P=9.3$ kbar. b) $Pb_{0.7}In_{0.3}$: 1) $P=0$; 2) $P=11$ kbar.

TABLE II. Shift of critical points of phonon spectra of metals and alloys under pressure.

Material	ω_t, meV	$\frac{d\ln\omega_t}{dP}$, 10^{-6} bar^{-1}	ω_l, meV	$\frac{d\ln\omega_l}{dP}$, 10^{-6} bar^{-1}	P_{max}, kbar	Ref.
Pb	a) 3,76	8,0±0,3	3,45	6,9±0,3	12,2	53, 104
	4,45	7,9±0,3				
	4,8	6,15±0,3				
	b) 3,8	7,4±1,9	8,45	7,1±0,7	10	11
	4,45	8±1,6				
	4,9	6,5±1,4				
	c) 4,56	6,1±8	8,66	6,2±7,2	17	19
Sn	a) 3,5	6,3	10,6	4	9	11
	4,8	4,6	14,2	3,9		
	7,6	6,5	15,9	4,2		
	b) 3,18	4,8±0,6	13,4	3,2±0,4	11	75
	4,64	4,8±0,6				
In	3,25	5±0,7				
	4,6	5,7±0,8	12,8	3,7±0,4	9,4	11
	—	7,4±0,7	—	3,9±0,2	16,7	18
	—	5,21±0,5				
Tl	3,99	3,7	9,5	5,45	9	69
Bi III	2,5	—				
	4,2	—	9,9	—	29	17
Nb	16,06	0	23,44	0,64±0,6	6	34
Ta	11,43	1,5±0,5	16,08	1,71±0,5	9	38
La	4,4	—4,55	8,8	0		20
			10,4	2,8	17,5	
In—Sn						
Sn, at. %: 3	3,1	5,65	13,41	4	9,3	86
	4,61	5,2				
11	2,8	1,8	13,75	1,1	9	86
	4,64	2,7	12,7	2,9		
23	3,39	5,5			4	86
$Pb_{0,95}In_{0,05}$	a) 3,68	8,6±0,3	8,52	6,8±0,3	10	53, 104
	4,4	8,4±0,3	9,57	6,1±0,3		
	4,78	7±0,3	9,78	5,8±0,5		
	4,526	7,52±0,71	8,65	5,83±0,21	3,6	16
$Pb_{0,88}In_{0,12}$	a) 3,52	9,1±0,5	8,62	6,1±0,3	9,5	53, 104
	4,3	7,0±0,5	9,76	5,3±0,3		
			10,36	4,0±0,5		
	b) 4,409	7,57±0,61	—	5,87±0,17	3,6	16
			—	4,62±0,22		
	c) 4,3	6,4±1,5	—	6±0,6	3,5	78
			—	4,3±0,6		
	3,22	7,8±0,3	8,71	5,5±0,3	11	53, 104
$Pb_{0,7}In_{0,3}$	4,2	6,0±0,3	10,15	4±0,3		
$Pb_{0,64}In_{0,36}$	3,67	6,1±1,4	8,79	5,56±0,6	3,5	78
			10,43	3,84±0,6		
$Pb_{0,6}In_{0,4}$	2,9	7,5±1	8,73	5,6±0,7	9,5	73
			10,7	2,7±0,7		
$Pb_{0,9}Bi_{0,1}$	3,1	4,8±1,4			11	105
	3,76	7,2±0,4				
	4,23	6,4±0,7	8	8,1±0,7		
	4,8	5,2±1,1	8,4	5,9±0,9	11	105
$Pb_{0,7}Bi_{0,3}$	2,8	13±3				
	3,4	7,1				
	3,85	6,2	8	6,3±0,6		
	4,8	—	8,35	4,8±0,6		
$Pb_{0.62}Bi_{0,38}$	2,78	9±2			11	105
	3,36	8,3±1,1	7,85	7,6±1,3		
	3,8	10,5±3,3	8,1	7,2±0,8		
	4,8	6,2±1,2	8,45	7,1±1,4		
Bi—Tl: ε phase	2,22	10,7±1			12	76
	3,8	7,7±1	8,8	6,8±0,6		
	5	4,5±0,6	9,68	5,1±0,6		
Bi_2Tl	1,98	7,6±1			12	76
	2,8	—				
	3,46	—				
	3,86	5,2±1	8,76	5,1±0,6		
	5,14	3,2±0,6	9,88	4,3±0,6		

sure the local vibrations would shift at the same rate as the upper limit of the phonon spectrum of lead. This is quite true of the experimental results obtained for alloys with low (1–7%) indium concentrations,[80] but it is in conflict with the observations on samples with high concentrations of the light indium impurity,[73] which we can reasonably attribute to a change in the force constants in the alloy.

On the whole, the reported results are evidence of complex changes in the phonon spectra of metals and alloys under pressure. Unfortunately, there is as yet no detailed theoretical description. For example, calculations of $\gamma_l(\mathbf{q})$ carried out by the pseudopotential method for several pure metals[81] give different relations between $\gamma_l(\mathbf{q})$ and $\gamma_t(\mathbf{q})$ for different values of $\mathbf{q}$, for example, in the case of lead the boundary of the Brillouin zone along the [111] direction we have $\gamma_l > \gamma_t$. On the other hand, as pointed out already, the tunnel experiments give the opposite inequality $\gamma_t > \gamma_l$ for practically all the investigated materials.

5.3. Interaction of electrons with the lattice

The knowledge of the spectral function of the EPI $g(\omega) = \alpha^2(\omega)F(\omega)$ is important for the description and understanding of the nature of the changes in superconducting properties.[82] This function represents the spectral dependence of the energy gap parameter $\Delta(\omega)$, which is a function of renormalization of the electron spectrum of a normal metal $Z_N(\omega)$, and can be used to calculate the EPI constant

$$\lambda = 2\int_0^\infty \frac{g(\omega)}{\omega}\,d\omega,$$

the Coulomb pseudopotential μ^*, and the changes in the mass and velocity of an electron near the Fermi surface $m^* = m[\mathrm{Re}\,Z_N(0)] = m(1+\lambda)$; it can also be used to calculate the integral characteristics of the EPI spectrum.

$$\langle\omega\rangle = \frac{2A^2}{\lambda}, \quad A^2 = \int_0^\infty g(\omega)\,d\omega,$$

$$\bar{E} = \int_0^\infty g(\omega)\,\omega\,d\omega = \frac{N(0)\langle J^2\rangle}{2M},$$

where $N(0)$ is the density of the electron states on the Fermi surface, $\langle J^2\rangle$ is the square of the matrix element of the electron-ion interaction. M is the mass of an ion, and also to find the critical temperature of a superconductor T_c, particularly using the approximate relationship[8]

$$T_c = \frac{\langle\omega\rangle}{1,2}\exp\left[-\frac{1{,}04(1+\lambda)}{\lambda-\mu^*(1+0.62\lambda)}\right]. \qquad (5.2)$$

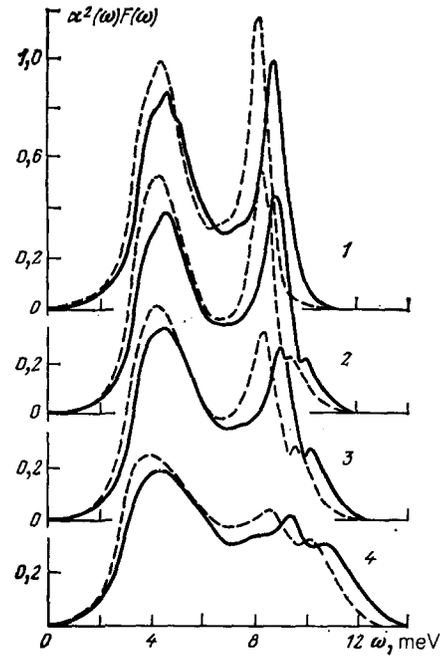

FIG. 11. Pressure-induced changes in the spectral EPI function of lead and its alloys with indium.[85] Here and in Figs. 12 and 20 the dashed curves correspond to $P = 0$; the continuous curves correspond to $P = 12$ kbar (curve 1, Pb), 10 kbar (curve 2, $Pb_{0.95}In_{0.05}$), 9.3 kbar (curve 3, $Pb_{0.88}In_{0.12}$), and 11 kbar (curve 4, $Pb_{0.7}In_{0.3}$).

The tunnel experiments are currently perhaps the only source of quantitative data on the function $\alpha^2(\omega)F(\omega)$. The procedures for reconstruction of the function $\alpha^2(\omega)F(\omega)$ from the tunnel data are well known[2] (see Sec. 2).

In the experiments carried out at the Donetsk Physicotechnical Institute the "dispersion" method[24–26] was used to obtain unconflicting and reliable data on the change in the EPI spectral function $\alpha^2(\omega)F(\omega)$ when pressures up to 14 kbar were applied to lead, indium, niobium, tantalum, alloys

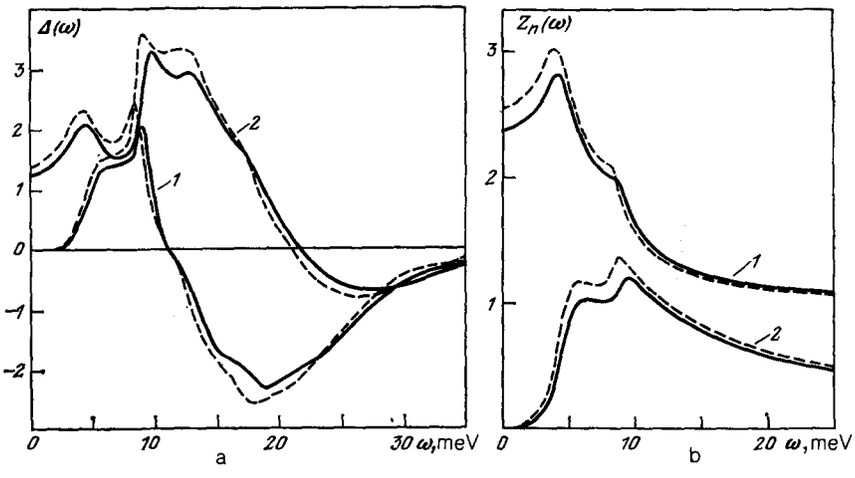

FIG. 12. Changes in the energy gap parameter (a) and in the renormalization function (b) of lead (the continuous curves were obtained for $P = 12.2$ kbar).[53] Here and later curves denoted by 1 are the real parts of the complex functions and the curves denoted by 2 are the imaginary parts.

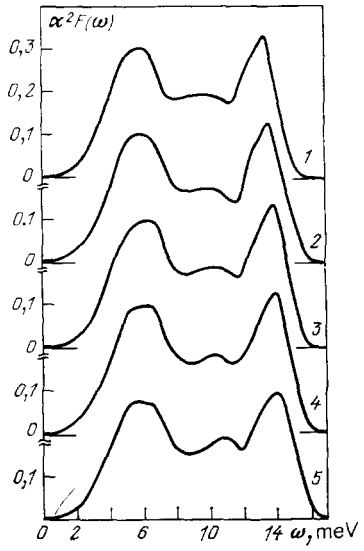

FIG. 13. Pressure-induced changes in the EPI function of indium.[75] P (kbar): 1) 0; 2) 3; 3) 5; 4) 7; 5) 10.

of bismuth in indium, indium with tin, and bismuth with thallium.[38,75,76,82–86] The experimental data for the superconducting modification Bi III ($P \sim 30$ kbar)[17] were also analyzed by this method.[3,87] An iteration procedure[47] was used in the experiments on lead and its alloys up to 3.5 kbar carried out at the Edmonton University in Canada and at the State University of New York, However, shortcomings of the reconstruction programs, inaccuracies in the initial experimental data, and the low range of pressures raise doubts about the quantitative aspects of these results. It has not been possible to reconstruct reliably the function $\alpha^2(\omega)F(\omega)$ for lanthanum under pressures up to 17.5 kbar (Ref. 20).

All this points to higher requirements in respect of the tunnel experiments at high pressures and the methods for analysis of the experimental data.

Our results were made reliable by investigating tunnel contacts in which nontunnel leakage currents were avoided, by employing a wide range of pressures in excess of 10 kbar, by the design of experiments ensuring reproducibility of the data for a large number of samples and reversibility of the properties after removal of the pressure, and by imposing rigid requirements on the experimental tunnel density of states and on the calculated data, as formulated in Ref. 88.

Typical pressure-induced changes of the parameters of the EPI function are plotted in Figs. 11–15 and are listed in Table III. The main result of these investigations is the reduction in the amplitude of the EPI function. It demonstrates, like the reduction in $2\Delta_0/T_c$ discovered earlier, that the EPI bcomes weaker on increase in the pressure. For all the investigated metals and alloys an increase in the parameter $\bar{E}$ was found by computer calculations. Within the limits of experimental error, the Coulomb pseudopotential was insensitive to changes in the lattice parameters in the investigated range of pressures. However, the value of this pseudopotential varied considerably for different materials.

5.3.1. Nontransition metals. The simplest model postulating constancy of the microscopic Grüneisen parameter describes qualitatively the change in the EPI functions of nontransition metals under pressure[21]:

$$g^{(P)}(\beta\omega) = \frac{B}{\beta^2}\, g^{(0)}(\omega), \tag{5.3}$$

where $g^{(P)}(\omega)$ and $g^{(0)}(\omega)$ are the EPI functions at finite and zero pressures; $\beta = 1 + \gamma\varkappa P$; γ is the macroscopic Grüneisen parameter; $\varkappa$ is the compressibility. The parameter $B(P)$ includes the changes in the electron chracteristics because of the compression of crystals and determination of this parameter presents a special problem.[23] A simple expression for the pressure dependence of B may be obtained on the basis of Ref. 89, where it is shown that the influence of the EPI in the case of nontransition metals is described sufficiently accurately by a simple analytic expression for the form factor of the unscreened pseudopotential $v_i(r) = C_1/r^2 - z/r$, where C_1 is a constant and z is the valence charge. Using the relationship for $B(P)$ from Ref. 21, we find that in this case we have $B = 1 + 1.2\varkappa P$. We can thus deduce the following relationships

$$\begin{aligned} \frac{d\ln\lambda}{dP} &= (1{,}2 - 2\gamma)\,\varkappa, \\ \frac{d\ln\bar{E}}{dP} &= 1{,}2\varkappa, \\ \frac{d\ln A^2}{dP} &= (1{,}2 - \gamma)\,\varkappa. \end{aligned} \tag{5.4}$$

In the case of lead we have $\gamma_{Pb} = 2.84$ (Ref. 90) and $\varkappa_{Pb} = 2.05 \times 10^{-6}$ bar^{-1} (Ref. 91), so that $d(\ln\lambda)/dP = -9.18 \times 10^{-6}$ bar^{-1}, $d(\ln\bar{E})/dP = 2.46 \times 10^{-6}$ bar^{-1}, and $d(\ln A^2)/dP = -3.36 \times 10^{-6}$ bar^{-1}. These calculated values are in excellent agreement with the experimental data for lead given in Table IV. Therefore, the knowl-

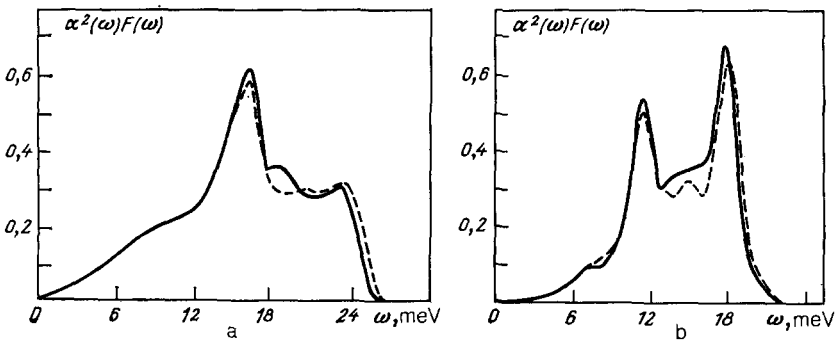

FIG. 14. Pressure-induced changes in the EPI functions of: Niobium (a, $P = 6$ kbar) and tantalum (b, $P = 9$ kbar).[38] The continuous curves correspond to $P = 0$ and the dashed curve to nonzero pressures.

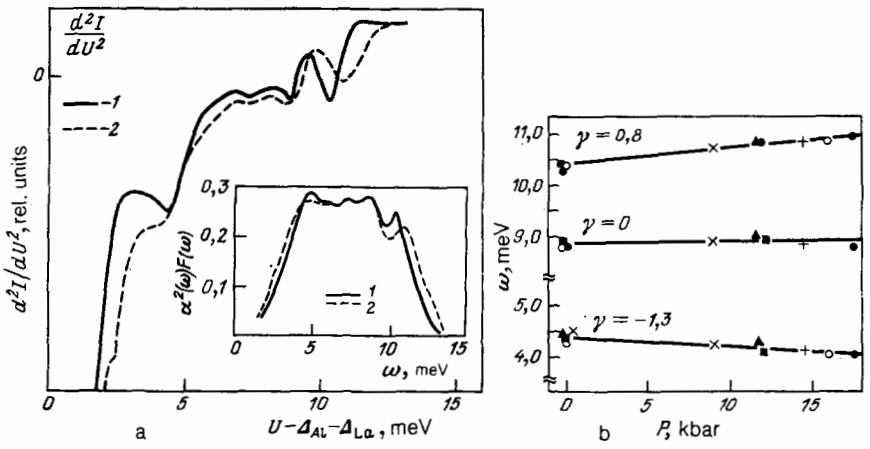

FIG. 15. Pressure dependences of the form of the d^2I/dU^2 curves (a) and of the characteristic Van Hove singularities (b) of lanthanum.[20] 1) $P = 0$; 2) $P = 17.5$ kbar. The inset in a shows the change in the EPI function of lanthanum as a function of energy at pressures 1 and 2.

edge of two macroscopic parameters γ and $\varkappa$ is sufficient for the satisfactory description of the influence of pressure on the EPI parameters of nontransition metals.

It is interesting to compare the results for $d(\ln\lambda)/dP$ with the experimental values of the coefficient $\gamma_e = (2/3)\pi^2 k_B^2 N(0)(1+\lambda)$, which governs the specific heat of a metal at low temperatures. According to the free-electron model, the density of electron states at the Fermi level is $d[\ln N(0)] = \varkappa/3$. It then follows from the data in Table III that in the case of lead we have $d(\ln\lambda_e)/dP = -4.9\times10^{-6}$ bar^{-1}. Other methods give the following values of the derivative $d(\ln\lambda_e)/dP$: $-(3.5\pm1)\times10^{-6}$ bar^{-1} (Ref. 9); $-(7.4\pm0.8)\times10^{-6}$ bar^{-1} (Ref. 92); $-(4.3\pm0.5)\times10^{-6}$ bar^{-1} (Ref. 93).

5.3.2. Niobium and tantalum. Attempts to investigate the EPI by the tunnel method in the case of films and single crystals have given anomalous values of the constant λ (the values were too small) and of the Coulomb pseudopotential μ^* (negative values). These results cannot be explained simply by the presence of a normal layer on the surface of a niobium single crystal near a barrier or by a structural defect, so that the existence of a nonphonon superconductivity mechanism has been suggested for niobium.[94]

The results of systematic tunnel investigations of the EPI in niobium and tantalum single crystals subjected to hydrostatic pressures were reported in Ref. 38. In the actual determination of the density of states in superconductors from the tunnel data an allowance was made for the dependence of the potential barrier transparency on the applied voltage. The nature of the spectral EPI functions of niobium and tantalum and their changes under pressure are presented Fig. 14. The values of λ and μ^* obtained by us together with the data of other authors[39] demonstrate that the superconducitivty of these transition metals is primarily due to the electron-phonon mechanism of the Cooper pairing of electrons. The calculated values of T_c are in good agreement

TABLE III. Influence of pressure on EPI parameters of superconductors.

Material	λ	meV^2	A^2, meV	d ln $\varkappa$/dP, 10^{-6} bar^{-1}			P_{max}, kbar	Ref.
				λ	$\bar{E}$	A^2		
Pb	1,553	23,2	3,945	—9,2	2,2	—3,4	12,2	53, 83
In	0,80	25,1	2,78	—8,5	2,35	—1	10	75
Bi III	1,48	27,47	5,4	—	—	—	29	76
La	0,82	—	—	—	—	—	17,5	20
Nb	0,9	92,28	5,87	0	0	0	6	38
Ta	0,68	61,07	4,32				9	38
In—Sn								
In, at. %:								
3	0,86	—	—	—10,4	—	—	9,3	86
11	1,08	—	—	—9,8			9	86
23	1,24	—	—	—12,3			4	86
Pb—In								
In, at. %:								
5	1,56	23,9	4,01	—7,8	1,3	—5,15	10	53, 104
	1,548	24,04	4,053	—6,91	2,086	—3,777	3,63	16
12	1,57	24,5	4,05	—8,2	2,7	—3,8	9,4	53, 104
	1,519	24,532	4,04	—7,926	2,479	—3,155	3,63	16
30	1,575	24,96	3,98	—8,14	3,2	—3,1	11	53, 104
36	1,42	—	3,893	—7,46	—4,26	—5,8	3,5	78
Pb—Bi								
Bi, at. %:								
10	1,67	22,6	4,02	—11,7	1,8	—4,6	11	84
30	2,08	23,7	4,5	—13,9	3,5	—4,8	11	84
38	2,11	25,0	4,6	—14,0	3,3	—4,4	11	84
$Bi_{0,6}Tl_{0,4}$	1,58	20,57	3,58	—14,7	3,5	—5	8,2	76
Bi_2Tl	1,65	22,39	3,78	—8,95	3,15	—3	8,8	76

TABLE IV. Superconductivity parameters T_c and $2\Delta_0$, and critical points ω_i of phonon spectra of Bi–Tl system[76].

Material	ε-phase					Bi_2Tl-phase				
	Tl	$Bi_{0.55}Tl_{0.45}$	$Bi_{0.58}Tl_{0.42}$	$Bi_{0.6}Tl_{0.4}$	$Bi_{0.62}Tl_{0.38}$	$Bi_{0.65}Tl_{0.35}$	$Bi_{0.68}Tl_{0.32}$	$Bi_{0.7}Tl_{0.3}$	$Bi_2Tl + BiI$ $Bi_{0.9}Tl_{0.1}$	Bi III [17]
$2\Delta_0$, meV	0,75	2,30	2,34	2,36	2,47	2,560	2,596	2,62	2,62	2,7
T_c, K	2,38	5,75	5,88	6,05	6,21	6,52	6,61	—	6,6	7,19
ω_t, meV 1	—	2,4	2,3	2,22	2,11	2,04	1,98	2	2,08	2,5
2	—	—	—	—	—	2,84	2,8	2,82	2,8	—
3	—	—	—	—	—	3,5	3,46	3,42	3,43	—
ω_l, meV 4	3,99	3,84	3,8	3,8	3,72	3,96	3,86	3,84	3,72	4,2
5	—	4,96	5	5	4,95	5,2	5,14	5,08	5,2	—
1	—	8,92	8,84	8,8	8,65	8,95	8,76	8,76	8,72	—
ω_l, meV 2	9,5	9,76	9,72	9,68	9,65	9,85	9,88	9,76	9,8	9,9

with the measurements. The difference between the behavior of the phonon spectra of niobium and tantalum under pressure, deduced from the shift of the characteristic transverse ω_t and longitudinal ω_l frequencies (Fig. 10), can be summarized as follows. In the case of niobium there is a stronger shift of the longitudinal vibration frequency, whereas in the case of tantalum the shifts are the same for both polarizations. In the investigated range of pressures the values of the Grüneisen parameter are $\gamma_{Nb} = 1.7$ and $\gamma_{Ta} = 1.94$. The data on $d(\ln T_c)/dP$ yield the following volume dependence of the electron parameter $S_e = d[\ln(N(0)\langle J^2\rangle)]/d(\ln \Omega)$: $S_e = -2.25$ for niobium and $S_e = -2.65$ for tantalum. The considerable changes in this parameter from one transition metal to another are due to the broadening of the *s-p* energy band under pressure and its upward shift on the energy scale.

It follows from these results that at low hydrostatic pressures the reduction in the critical superconducting temperatures of niobium and tantalum is mainly due to changes in the vibrational spectra of their lattices.

5.3.3. Lanthanum. In contrast to niobium and tantalum, the application of pressures up to 17.5 kbar to lanthanum[20] results in softening ($\gamma_i^* < 0$) of transverse phonon models (Fig. 15). This in turn increases the gap in the critical temperature T_c, so that the ratio $2\Delta_0/T_c$ rises from 3.75 for $P = 0$ to 4.6 for $P = 17.7$ kbar. The inequality $|d(\ln \Delta_0)/dP| > |d(\ln T_c)/dP|$, discovered for simple metals, is still obeyed. These experimental results do not confirm the earlier hypothesis of other (apart from EPI) pairing mechanisms in lanthanum, for example, the so-called "4*f*-electron mechanism." It has been postulated theoretically that the applied pressure raises the 4*f* band and this reduces μ^* and increases T_c. It follows from the tunnel results that the softening of phonons and the enhancement of the EPI are another important and realistic reason for the increase in T_c. This mechanism has not been considered before. An analysis of the results obtained has led to the conclusion[20] that an increase in the density of states in the 4*f* band of lanthanum softens phonons under pressures and also gives rise to a low Deybe temperature and a low melting point.

It is interesting that the calculations of Ref. 95 demonstrate reduction in the average phonon frequency and an increase in the strength of the EPI in lanthanum on increase in the applied pressure up to 35 kbar when a phase transition possibly takes place.

5.4. Critical temperature of the superconducting transition and calculations of electron-phonon interaction parameters

The Eliashberg equations at $T = 0$ and $T = T_c$ are the limiting cases of the relationships obtained in the "temperature" technique for arbitrary temperatures. Therefore, it is possible to calculate the critical temperature of a superconductor from exact relationships using the EPI functions deduced from the tunnel experiments.

Physically such calculations represent a test of the reliability of the reconstructed EPI functions and they make it possible to estimate critically the accuracy of some of the semiempirical formulas for T_c [for example, Eq. (5.2)]. In contrast to the exact solutions, such formulas predict a much smaller shift of T_c under pressure: the shift should be by 20–40% in accordance with Eq. (5.2) and by 10–15% in accordance with the variant of Eq. (5.2) improved in Ref. 96. This conclusion is independent of the errors in the determination of pressures and it follows from the integral characteristics of the same EPI functions which are used in the exact calculations of T_c.

In addition to rigorus calculations of T_c, there is another way of checking the EPI function. It involves a determination of the tunnel density of states at energies exceeding the limit of the phonon spectrum of a given metal. The results of such a comparison in the range in excess of 11 meV for lead and in excess of 14 meV for some lead-indium alloys at finite pressures (the calculations were made using the experimental values only up to these pressures) are plotted in Fig. 16. These results demonstrate agreement between the "rigorously" calculated and experimental values of T_c and they also show convincingly that the microscopic theory is suitable for the description of superconducting properties of nontransition metals under pressure.

We can see that the experimental data on the function $\alpha^2(\omega)F(\omega)$ can be used to describe completely the observed pressure-induced changes in the superconducting properties of metals. In the case of the mechanisms of changes in the spectral EPI functions, it is particularly valuable to carry out calculations of the main EPI characteristics from first principles. Unfortunately, such calculations have been carried

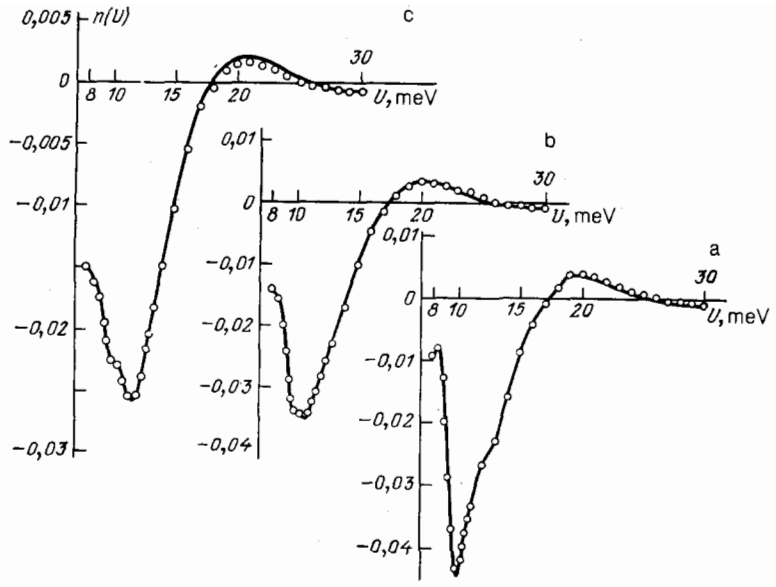

FIG. 16. Comparison of the calculated (continuous lines) and experimental (circles) tunnel densities of states.[52] a) Pb, $P = 12.2$ kbar; b) $Pb_{0.88}In_{0.12}$, $p = 9.3$ kbar; c) $Pb_{0.7}In_{0.3}$, $P = 11$ kbar.

out so far only for simple metals. By way of example, we shall mention Ref. 97 where a study is reported of the influence of hydrostatic pressures on the renormalization of the effective mass of an electron in sodium and potassium. A consistent allowance for the relevant factors (changes in the and mass of an electron, in the electron-phonon coupling constant, and in the corresponding parameter describing the contribution of the electron-electron interaction) has made it possible to establish that there is a disagreement between the theoretical and experimental values of $d(\ln m^*)/dP$ for these metals.

The progress made in the calculations of the EPI parameters of various metals, alloys, and compounds (particularly of transition metals[98]) allows us to hope that similar results will be obtained also at high pressures. It is essential to allow for real factors that affect the EPI in the investigated materials: disorder of the investigated materials, especially superconducting alloys,[99] anisotropy of the electron-phonon characteristics,[100,101] and amorphization.[102]

6. TUNNELING IN SYSTEMS WITH COMPOSITIONS CLOSE TO PHASE EQUILIBRIUM BOUNDARIES

Studies of multicomponent systems are of considerable interest. The pressure and impurities can induce different phase states and a lattice instability favoring one of the phases may appear near a phase transition.[98] Therefore, we are naturally faced with the question whether the actual design of the tunnel experiments on such complex multiphase objects is the correct one at high pressures and low temperatures when structural transitions can take place in the material during measurements.

6.1. Lead-bismuth system

In the broad investigated range of compositions of lead-bismuth alloys there are various phase states.[103] At temperatures below the eutectic value some of the homogeneous regions are separated by two-phase mixtures. For example, at room temperature and under normal pressure the alloys of lead with bismuth containing less than 18 at. % Bi are substitutional solid solutions with the fcc structure of lead (α phase). A further increase in the amount of bismuth in lead gives rise in the 28–34 at. % Bi range to a homogeneous region of an intermediate ε phase (hcp lattice) adjoining two-phase regions $\alpha + \varepsilon$ and $\varepsilon + \alpha'$, where α' (or Bi) is a solid solution based on bismuth.

The results of the tunnel experiments showed that the tunnel current is sensitive to a change in the phase composition.[84,104,105] Figure 17 gives the tunnel characteristics of the lead-bismuth system obtained in the range of voltages $U = \Delta_{Pb-Bi} \pm \Delta_{Al}$ applied to the barrier when different

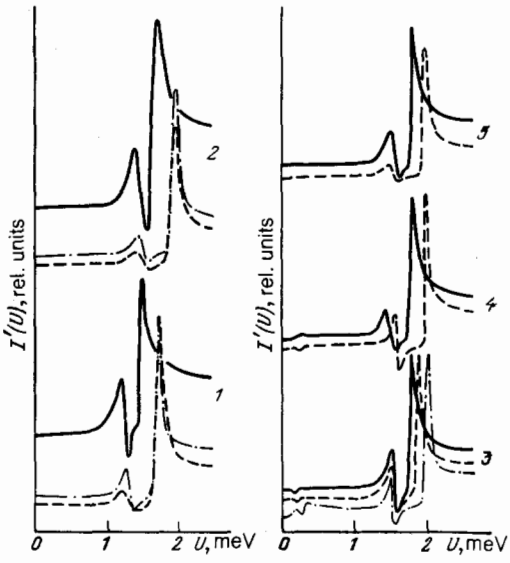

FIG. 17. Influence of annealing under pressure on the tunnel conductance of lead-bismuth systems.[104] Bi content (at. %): 1) 10; 2) 30; 3)-5) 38. The dashed curves represent the initial data and the continuous curves are the results obtained at different pressures P (kbar): a), 2) 11.8; 3)-5) 10. The chain curves represent 6 kbar (curves 3–5) and the drop to 0.8 kbar (curves 1 and 2). The family of curves denoted by 3 represents samples cooled rapidly immediately after compression; the family of curves 4 represents samples annealed at room temperature for 3 days at $P = 4$ kbar; the family of curves 5 denotes samples annealed for 20 days at $P = 10$ kbar.

phase states are observed at high hydrostatic pressures. In the case of single-phase solutions containing 10 and 30 at. % Bi (dependences 1 and 2) the tunnel conductivity is typical of homogeneous pure superconductors (compare with Figs. 1a and 6). The situation changes drastically in the case of a two-phase mixture with the bismuth concentration 38 at. % (dependences 3–5). The proximity of undissolved bismuth to the superconducting phase induces an energy gap in this phase and gives rise to singularities in the conductance at low voltages $U = \Delta_{Al} \pm \Delta_{Bi}$. Prolonged storage of samples at room temperature at a fixed pressure and the subsequent immersion in a cryostat alters the characteristics because of a redistribution of the actual amounts of the phases. The conductance singularities corresponding to the tunneling to the Bi phase become weaker (curve 4 in Fig. 17) and finally disappear completely (curve 5 in Fig. 17). Such a change is due to an additional solubility of the excess bismuth in the ε phase, as a result of which there is a shift of the $\varepsilon \rightleftarrows \varepsilon + \text{Bi}$ equilibrium in the direction of Bi. This result is not in conflict with the theoretical phase diagram of the lead-bismuth system under pressure.[106] We can see from Tables I and III that an increase in the solubility of bismuth because of the shift of the phase equilibrium boundary under pressure gives rise to a single-phase superconductor $Pb_{0.62}Bi_{0.38}$ with a high critical temperature $T_c = 9$ K and a strong EPI ($\lambda = 2.11$). The corresponding EPI functions are presented in Fig. 18. It follows from these experiments that the tunnel spectroscopy can be used together with other methods in studies of phase transitions.

On the other hand, the tunneling to a superconducting multiphase structure, representing an object with a strongly inhomogeneous distribution of the order parameter, presents a different problem. In the calculations of the one-particle current flowing into such an inhomogeneous system we meet with difficulties due to the need for statistical averaging and for averaging over the random distributions of the phases. The distribution functions in turn are governed by the conditions of formation of a film, the dispersion of the individual phases, and the degree of their mutual ordering. The experimental characteristics of two-phase objects[104] are in many ways analogous to those of layer structures[107] for which there are some well-tested theoretical models.[40,43] Therefore, the approach to the tunnel effect in a multiphase system should be based on the ideas of the proximity effect and on the flow of parallel tunnel currents to different phases.

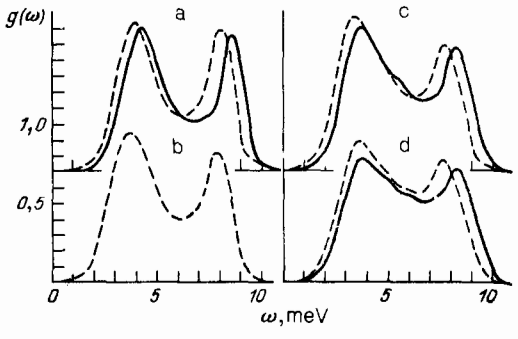

FIG. 18. Pressure-induced changes in the EPI function of lead-bismuth alloys.[105] a), b) $Pb_{0.9}Bi_{0.1}$ and $Pb_{0.8}Bi_{0.2}$, $P = 10$ kbar; c), d) $Pb_{0.7}Bi_{0.3}$ and $Pb_{0.62}Bi_{0.38}$, $P = 9.5$ kbar; b, d) data obtained at $P = 0$ for samples quenched from $T \approx 380$ K and at $P \neq 0$ after storage at room temperature under pressure of $P = 14$ kbar for 40 days.

6.2. Bismuth-thallium system

According to the phase diagram of Ref. 103 the middle range of compositions (55–63 at. % Bi) exhibits at $P = 0$ an ε phase with a hexagonal structure and three atoms per unit cell. The chemical compound Bi_2Tl is outside the ε phase in the diagram, i.e., this compound is unstable at atmospheric pressure and room temperature. When the pressure is in excess of 5 kbar, all the alloys between 62 and 85 at. % Bi show splitting of the eutectic transition line into two lines, indicating the existence of intermediate phases.

In contrast to the alloys of lead with bismuth and indium, the fine structure of the phonon spectrum of bismuth-thallium alloys is readily resolved by plotting the second derivatives of the current-voltage characteristics (Fig. 19). This is due to the ordered distribution of atoms between the lattice sites and slight fluctuations of the interatomic forces in the system. The addition of bismuth results in major changes in the low-frequency part of the phonon spectrum: new singularities appear (2.8 and 3.5 meV). Their appearance is preceded by some softening of the low-frequency mode from 2.4 to 2 meV, which is accompanied by an increase of T_c at the ε phase boundary from 5.8 to 6.6 K and by an increase in $2\Delta_0$ from 2.3 to 2.6 meV (Table IV).

In the experiments under pressure (3.6, 4.8, 8, 11, and 12 kbar) the superconducting parameters Δ_0 and T_c decrease and this effect is stronger for the ε phase (see Tables I and III). The positions of the characteristic frequencies in the phonon spectra shift toward higher energies and this is typical of all the bismuth concentrations. However, all the samples with the bismuth content in excess of 65 at. % demonstrate disappearance of the points $\omega_i^{(2)} = 2.8$ meV and $\omega_i^{(3)} = 3.5$ meV at pressures higher than 3.7 kbar, which probably reflects creation of a new intermediate phase of

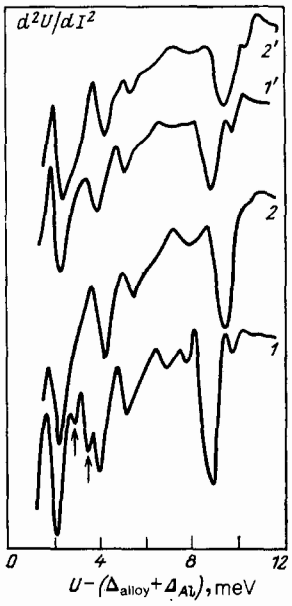

FIG. 19. Influence of pressure on the phonon structure of the bismuth-thallium system.[76] Bi_2Tl (curves 1 and 2) and ε phase (curves 1′ and 2′), 1), 1′) $P = 0$; 2), 2′) $P = 12$ kbar.

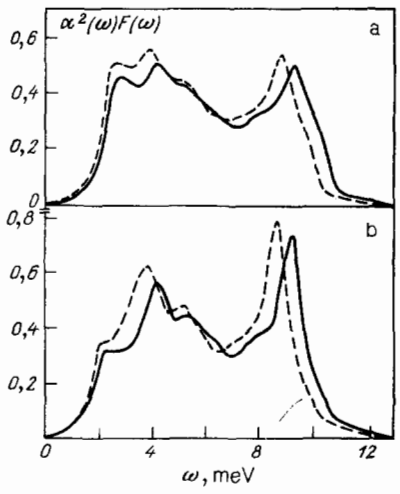

FIG. 20. Pressure-induced changes in the EPI function of the bismuth-thallium system.[76] a) $P = 8.2$ kbar, ε phase; b) $P = 8.8$ kbar, Bi_2Tl.

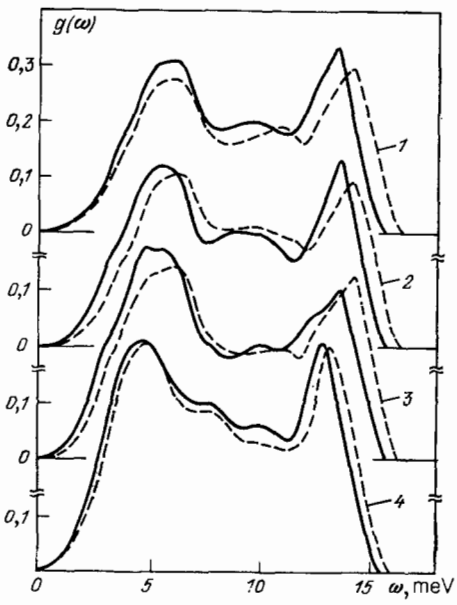

FIG. 21. Influence of pressure on the EPI functions of indium and its alloys with tin.[86] 1) In, $P = 10$ kbar; 2) $In_{0.97}Sn_{0.03}$, $P = 9.3$ kbar; 3) $In_{0.89}Sn_{0.11}$, $P = 9$ kbar; 4) $In_{0.77}Sn_{0.23}$, $P = 4$ kbar. The continuous curves correspond to $P = 0$ and the dashed curves to nonzero pressures.

Bi_2Tl. The effective phonon spectra of these phases (Fig. 20) differ considerably in respect of the ratio of the amplitudes, reflecting the role of the electron density in the formation of these spectra.

The measured tunnel characteristics and T_c of a large number of samples with different compositions indicate that the homogeneity range of the film condensate extends up to 70 at. % Bi and this is followed by a two-phase region. On the other hand, the dependences of d^2U/dI^2 on U do not change significantly in the phonon energy range and remain similar to those for the single-phase system for alloys with up to 67–70 at. % Bi. Consequently, we can ignore precipitation of pure bismuth, which would have created the singularities mentioned earlier in the tunnel spectra. This interpretation is supported by the results of an x-ray diffraction study of the same system under pressures of the order of 30 kbar (Ref. 108) which indicate that the solubility of bismuth in this system is observed only when it assumes the metallic state Bi III ($P \sim 29$ kbar). However, the pressures (from 3 to 4 kbar, depending on the composition) at which the singularities $\omega_t^{(2)}$ and $\omega_t^{(3)}$ disappear are much lower than the pressures corresponding to the Bi I → Bi II → Bi III transitions.

These results suggest also a relationship between the effects of the interaction between the Fermi surface and the Brillouin zone on the ordering processes. In this case it is interesting to consider several published experimental observations of the anomalies in the behavior of T_c and of the lattice parameters of the cubic lead-thallium and bismuth-thallium systems, which occur when the electron density is 3.5 electrons/atom. Attention is drawn in Ref. 109 to anomalies in the phonon spectrum at 4.18 electrons/atom near the fcc-hcp phase transition. However, a detailed analysis of this topic is not yet possible because of the absence of the energy band calculations for the intermetallic compound.

6.3. Indium-tin system

The crystal lattice of indium has normally the face-centered tetragonal (fct) structure and at room temperature the tegragonality parameter is $\delta = c/a - 1 = 0.078$ (here, a, and c are the lattice parameters). The addition of an impurity with a higher valence (tin) first increases the tetragonality parameters, but on approach to the boundary of the α phase this parameter falls. A further increase in the tin concentration to 12 at. % results in the $\alpha \rightleftarrows \beta$ transition which is accompanied by a small discontinuous change in the unit cell volume. The β phase also has the fct structure, but in contrast to the α-In phase it is characterized by the ratio $c/a < 1$. A characteristic feature of the α phase alloy is the occurrence of anomalies of some of the physical properties due to the electron-topological transitions in the system.[75]

The spectral EPI functions and their changes under pressure are plotted in Fig. 21 (Ref. 86). An increase in the electron density in these alloys increases T_c, Δ_0, $2\Delta_0/T_c$, and the EPI constant λ. This is due to an increase in the density of the electron states on the Fermi surface, which both increases the electron contribution to the constant λ and causes softening of the phonon spectrum (Table III).

When the electron density is increased, the spectral EPI functions are not only shifted but they show an increase in the peak amplitudes, as well as broadening and deformation of these peaks, particularly in the case of alloys close to the boundary of the α phase. These distortions are evidence of the appearance in the phonon spectrum of a group of frequencies characteristic of the β-phase alloys and they demonstrate the presence of an admixture of another phase. Hydrostatically compressed alloys in the $\alpha \rightleftarrows \beta$ transition region exhibit a more symmetric form of the EPI function, which would suggest a shift in the solubility limit of the α phase under pressure.

The electron and lattice contributions to the observed regular changes of T_c of the alloys were determined and reported in Ref. 79 The partial contributions due to introduction of the impurity were found to be as follows: 20% due to electrons and 80% due to the lattice in the α phase, with the corresponding values 83 and 17% for the β phase. The electron contribution to the change in the EPI constant under pressure was found to be $\sim 20\%$.

In the vicinity of the $\alpha \rightleftarrows \beta$ phase transitions there are

considerable and irregular changes in Δ_0, $2\Delta_0/T_c$, and in the frequencies ω_i which reduce to the following: this phase transition is preceded by softening of the phonon spectrum (particularly noticeable for ω_t), a rapid increase in the electron parameter $\bar{E}$, and a local rise of the ratio $2\Delta_0/T_c$ (Ref. 79).

6.4. Nonlinear changes in the energy gap and phonon spectrum of indium

In 1960, I. M. Lifshitz predicted the appearance of singular corrections to the thermodynamic potentials as a result of changes in the topology of the Fermi surface under the influence of impurities or pressures.[110] A method for detection of an electron-topological transition by a study of its influence on T_c, proposed and developed by B. G. Lazarev and his colleagues,[111] has proved to be very effective. This approach is based on the Makarov-Bary'yakhtar theoretical model which establishes the relationship between T_c and changes affecting small parts of the Fermi surface.[112] In the case of indium and its alloys with tin (α phase) there are electron-topological transitions[113] at low pressures ($P = 4$–6 kbar) and low impurity concentrations ($c = 1$–3 at. % Sn).

Detailed systematic investigations of the tunnel spectra of indium-tin alloys and of pure indium under pressure have revealed slight but fully noticeble nonlinear changes in the phonon frequencies.[114,115] The anomalous shift of the singularities in the tunnel spectrum under pressure is found to be very sensitive to the addition of the high-valence tin, stressing the relationship between the observed anomalies and the electron structure. These experimental results have stimulated a theoretical analysis of this topic.[116]

The physical nature of the nonlinear changes in the tunnel spectrum near an electron-topological transition is not yet fully understood. A. A. Galkin *et al.*[114] put forward the hypothesis that a lattice instability giving rise to a polymorphic phase transition appears in the vicinity of an electron-topological transition. The same conclusion was reached independently by L. Dagens,[117] He used the quasiharmonic adiabatic approximation to determine theoretically the behavior of the phonon spectrum of a metal in the case of an electron-topological transition. It was found that the nonanalyticity of the density of electron states near the critical value ε_c in the range $\varepsilon_F < \varepsilon_c$ is responsible for an irregular change in the average phonon frequency[109] and an anomalous correction to the free energy of phonons. The latter makes a metal unstable at low temperatures and can produce an isomorphic phase transition.[117]

7. ELECTRON SPECTROSCOPY

When the mean free path of the tunneling electrons becomes comparable with the distance between the boundaries of the investigated film, one has to take size effects into account. The basis of the effects described below is the quantization of energy levels in thin films and interference between electron waves reflected from the film boundaries. When certain specific conditions are satisfied, the tunnel conductivity exhibits a system of equidistant maxima and the separation between them (oscillation period) determines the velocity of carriers, whereas the nature of attenuation of these maxima carries information on some points in the energy band structure of a metal and on the state of the surface of a film.

7.1. Quantum size effect in metal films

The simplest of the size effects is the formation of electron waves in a thin film of thickness d regarded a a potential box. Interference between two electron states with the momenta p_x and $-p_x$ gives rise to quantum energy levels in the spectrum of the film:

$$\varepsilon = \varepsilon\left(\frac{\pi m\hbar}{d},\ p_y,\ p_z\right);$$

here m is an integer, $p = 2\pi\hbar/\lambda_F$, and λ_F is the de Broglie wavelength. Lifshitz and Kosevich[118] were the first to consider this situation in two-dimensional systems and the appearance of the corresponding oscillations of the tunnel current considered as a function of the voltage across the barrier was analyzed by Gogadze and Kulike.[119]

Observation of such quantized energy levels is possible if the irregularities of the film surface are small compared with the de Broglie wavelength. The most convenient objects for such investigations are naturally semiconductors and semimetals characterized by a low Fermi energy and a long electron wavelength. Therefore, the first reliable experimental proof of the existence of the quantum size effect was reported for bismuth, which is characterized by $\varepsilon_F \sim 10^{-2}$ eV and $\lambda_F \sim 10^{-5}$ cm (Ref. 120).

In the case of metals, until recently it has been thought (apparently justifiably) that the quantum size effect cannot be observed. In fact, because the Fermi energy is high, $\varepsilon_F \sim 10$ eV, the de Broglie wavelength is of the order of one interatomic distance $a \sim 10^{-8}$ cm. Formation of a film of such a small thickness free of defects is beyond the possibilities of present-day experimental physics. Nevertheless, the quantum size effect in metals has been observed[121] and systematic studies of this effect have been made under hydrostatic pressure conditions on films of thickness 200–600 Å (Refs. 122–124).

For the purpose of understanding the quantum size effect in metals it is important to remember that the thickness of real films varies in discrete steps amounting to one lattice parameter a: $d = Na$ (N is an integer). In fact, metal films consist of many blocks of different thickness and with a perfect crystal structure.[125] Such an experimentally unavoidable inhomogeneity of the films naturally hinders the observation of the quantum size effect, because each block or crystallite, depending on its thickness, has it own set of energy conditions

$$p_x^{(m)} = \frac{\pi\hbar m}{d}; \tag{7.1}$$

here x is the normal to the surface of the sample coinciding with the direction of the tunnel current. However, because d is discrete, there are always special points in the band structure which correspond to "codimensional" levels, i.e., levels which are the same for a large number of crystallites in a film. For example, an electron state with the momentum projection $\bar{p}_x = \pi\hbar/2a$ will be a resonance state for any block with an even value of N, because we can always find such a value of $m = N/2$ that

$$p_x^{(m)} = \frac{\pi\hbar}{a}\frac{m}{N} = \frac{\pi\hbar}{2a}. \tag{7.2}$$

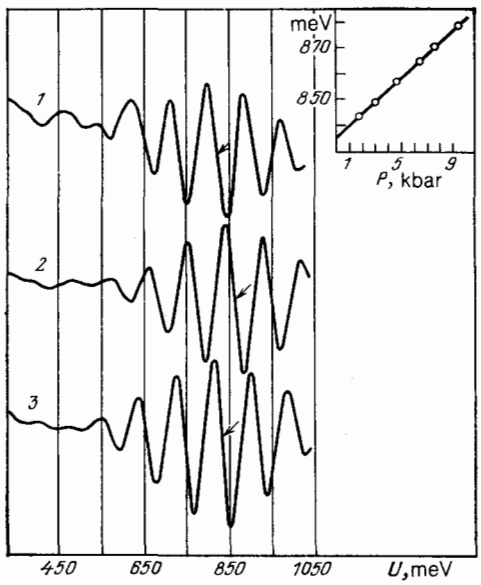

FIG. 22. Influence of pressure on the quantum size effect in a lead film[122] of thickness $d_{Pb} \approx 250$ Å: 1) $P = 0$; 2) $P = 10$ kbar; 3) drop of pressure to 1.5 kbar. The inset shows the shift of the central maximum.

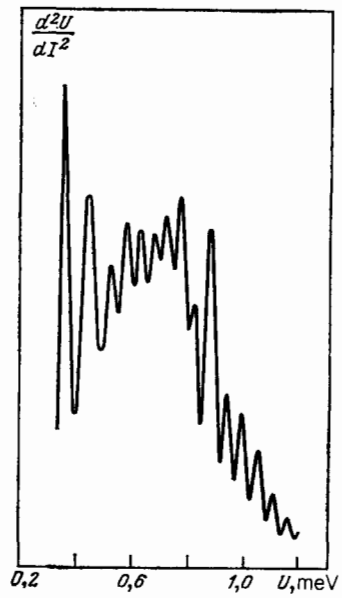

FIG. 23. Quantum size effect in polytextured lead films ($P = 0$).[122,124]

It is around such an energy level $\varepsilon(p_x, 0, 0) = \bar{\varepsilon}$ that oscillations of the tunnel conductivity with a period $\Delta\varepsilon = \pi\hbar v_0/2d$ are concentrated; v_0 is the group velocity (Fig. 22). The resonance electron levels adjoining $\bar{\varepsilon}$ decay rapidly away from $\bar{\varepsilon}$. An analytic description of the oscillations of the current was obtained in Ref. 122. We can see that an experimental investigation of the quantum size effect makes it possible to determine the values of some of the special points in the band structure of a metal and the group velocity of electrons at these points. The effect is manifested irrespective of the transitions of a material to the superconducting state.

Aluminum-aluminum oxide-lead contacts were investigated under pressure.[122–123] An x-ray structure analysis showed that lead films exhibited a well-developed structure and a preferential orientation along the [111] direction. Under normal pressure the center of the oscillation structure (curve 1 in Fig. 22) was located at $\bar{U} = \bar{\varepsilon} - \varepsilon_F = 0.82 \pm 0.02$ eV, in agreement with the theoretical value of 0.88 eV for lead.[126] Compession of a sample resulted in an increase in $\bar{U}$ at a rate $d(\bar{\varepsilon} - \varepsilon_F)/dP = 4.0 \pm 0.2$ meV/kbar. There was also an increase in the oscillation period:

$$\frac{d \ln(\Delta\varepsilon)}{dP} = (1.6 \pm 0.4) \cdot 10^{-6} \text{ bar}^{-1}. \qquad (7.3)$$

As expected, in the case of the states far from the Brillouin zone boundary the above value was close to 1.37×10^{-6} bar^{-1} calculated using the free-electron model.

The energy band structure of lead can be probed along other crystallographic directions by a method postulating that thin metal films exhibit a polytexture.[125] Although the conditions for the appearance of polytextures are difficult to control, nevertheless such samples have highly reproducible values of the energies at the oscillation maxima: $\bar{U}_i = 0.55$, 0.82, and 0.92 eV (Ref. 124), which are in satisfactory agreement with the calculations[126] of the energy band structure of lead along the [110], [111], and [100] directions, respectively. Figure 23 shows an example of a superposition of standing electron waves as a result of tunneling along different crystallographic directions to textured parts of a film. For $\bar{U}_{[110]} = 0.55$ eV the change under pressure was $d(\bar{\varepsilon} - \varepsilon_F)/dP = (3.9 \pm 0.2)$ meV/kbar. The experimental values of $d(\bar{\varepsilon} - \varepsilon_F)/dP$ made it possible to determine the derivative $d\varepsilon_F/dP$. In fact, in the case of electron states of energy $\bar{\varepsilon}$ located in the middle of the Brillouin zone it was found that, to within a few percent, one can apply the free-electron approximation and, therefore, $d\bar{\varepsilon}/dP = (2/3)\bar{\varepsilon}\varkappa$. It follows from the above results for lead that $d\varepsilon_F/dP = 10$ meV/kbar. This is approximately 75% less than the corresponding value obtained in the free-electron model.

Another method for the observation of the size effect far from resonance levels in metal films utilizes interference between two states with very similar values of the momenta, such that $|p_x' - p_x''| \ll p_F$. Then, the wavelength of interference excitation is much greater than the inhomogeneities of a sample. This effect is observed on tunneling near singularities of ε_c, particularly to small electron groups,[127] and on the basis of the Andreev reflection from the boundary between a superconductor and a normal metal.

7.2. Effects of the Andreev reflection of electrons

It is known that a state with a given energy in a superconductor is fourfold degenerate in respect of the momentum, i.e., one excitation energy ε corresponds to two quasielectron (with momenta p_+ and p_-) and two quasihole (with momenta q_+ and q_-) states. We shall consider an SIS(N) contact. An electron with a momentum p_+ tunneling to the S layer is reflected by the boundary with the normal metal and is scattered to a quasihole state with a momentum q_+, which is close to p_+: $(p_+ - q_+) \ll p_F$ (this effect was predicted by A. F. Andreev[128] and is known as the Andreev reflection). A superpositon of the two states creates a new excitation with a wavelength considerably greater than the Fermi value, since this new excitation carries a very small momentum $\hbar k \ll k_F$. In fact, two standing waves are established in the sample and they are characterized by $\Lambda = 2\pi/q$ and $\lambda_F = 2\pi/k_F$ ($\Lambda \gg \lambda_F$). These standing waves are very weak and they are manifested only in thin films (see

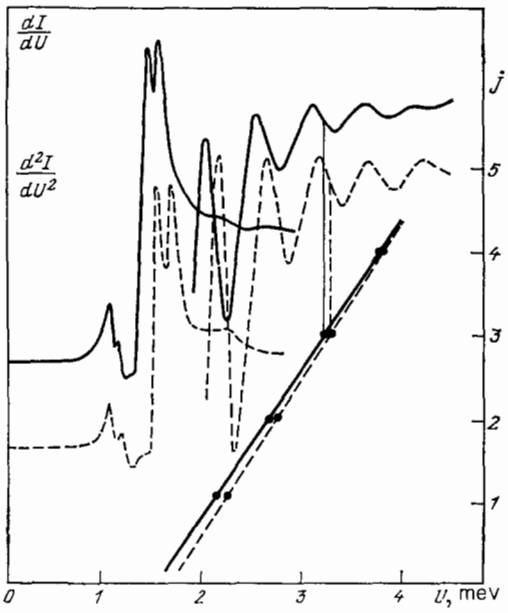

FIG. 24. Influence of pressure on the Andreev-Tomasch effect.[130] The continuous curves correspond to $P = 9$ kbar and the dashed curve to $P = 0$. The straight lines are the dependences of the oscillation period on the oscillation number for a film thickness $d_{Pb} = 3\times10^{-4}$ Å.

Sec. 7.1). Creation of new long-period waves is manifested in the tunnel conductivity of thick (d_S of the order of several microns) superconducting films covered by a normal metal. The positions of the minima of the resultant oscillations are given by the relationship[29]

$$U_n = \Delta_1 + \left[\Delta_0^2 + \left(\frac{\pi\hbar v_F^* n}{d_S}\right)^2\right]^{1/2} \quad (n = 1, 2, \ldots), \quad (7.4)$$

where Δ_1 is the gap of the injector and Δ_0 is the gap of the investigated material. These oscillations differ from those considered earlier (see Sec. 7.1) because they are in the zone of influence of the EPI and were discovered by W. J. Tomasch.[129]

A study of the influence of pressure on this effect was reported in Ref. 130. Tunnel contacts of the Al–I–Pb(Ag) type were investigated at 1.4 K (Fig. 24). Lead films with a strong texture along the [111] direction were $(2.5–3.2)\times10^4$ Å thick and silver films were approximately 10^3 Å thick. The pressure altered the tunnel characteristics because it reduced the energy gaps Δ_0 and Δ_1 and increased the oscillation period. The experimental dependence of the period on the oscillation number was a straight line with a slope that varied with the direction, reflecting an increase in the Fermi velocity of quasiparticles. After averaging a large number of the experimental results it was established that

$$\frac{d\ln(v_F^*/d_S)}{dP} = (7.7 \pm 0.7)\cdot10^{-6}\ \text{bar}^{-1}. \quad (7.5)$$

The derivative $d(\ln v_F^*)/dP \approx 7\times10^{-6}\,\text{bar}^{-1}$ obtained for lead was relatively large because of the influence of the EPI, which renormalized strongly the electron spectrum of this material. It was found that $v_F^* = v_F/Z_N(0)$, where v_F is the group velocity of quasiparticles on the Fermi surface found ignoring the EPI and $Z_N(0)$ is the renormalization coefficient. Since along the [111] direction in lead the value of $d(\ln v_F)/dP$ in the vicinity of the Fermi energy depends very weakly on the electron energy,[130] we can describe $d[\ln(v_F/d_S)]/dP$ using the result of Eq. (7.3) deduced from the quantum size effect data. Then, the renormalization coefficient of the spectrum is

$$\frac{d\ln Z_N(0)}{dP} = -(6.1 \pm 1.1)\cdot10^{-6}\ \text{bar}^{-1}. \quad (7.6)$$

This result is in full agreement with the data deduced by reconstruction of the function $g(\omega)$ (see Sec. 7.1) and both sets of results stress the dominant role of the weakening of the role of the EPI in the changes of the parameters of a superconductor under pressure.

Similar singularities were observed also on tunneling to a normal metal covered by a superconducting film (N/S contact). However, in contrast to a superconductor, the electron and hole states in an N layer do not interfere with one another so that reflection is needed for the addition of two electron waves: incident and reflected. Consequently, the positions of the oscillation maxima of the tunnel conductivity of NIN(S) structures with a normal injector are given by the same equation (7.4) with $\Delta_1 = \Delta_0 = 0$ and with d_S replaced with $2d_N$ (Ref. 47):

$$U_n = \frac{\pi\hbar v_F n}{2d_N} \quad (n = 1, 2, \ldots). \quad (7.7)$$

This was observed experimentally by J. M. Rowell and W. L. McMillan.[47]

These oscillations lie within a fairly narrow energy interval near $U = 0$ when the thickness of the normal layer d_N is large (several microns). If d_N is of the order of several thousands of angstroms, they cover the range of phonon frequencies of the superconductor and the conductivity of an NIN(S) structure is described by the usual tunnel characteristic of Eq. (2.4) in the case when $U \gg \Delta_0$, and this conductivity is modulated by an oscillatory function with a period governed by the Fermi velocity of electrons v_F in the normal metal[47]:

$$\sigma(U) = \sigma_0\left\{1 + \text{Re}\left[\frac{\Delta_S^2(U)}{2U^2}\int_0^\infty \exp\left(\frac{i4Ud_Nx}{\hbar v_F}\right)\frac{dx}{x^2}\right]\right\}. \quad (7.8)$$

The possibility of investigating the electron spectra of normal metals under pressure was discussed in Ref. 131, where a study was reported of the differential conductivity of Al–I–Ag(Pb) structures with $d_{Ag} = 1500–4500$ Å and $d_{Pb} = 3000$ Å at 1.4 K. An analysis of the observed oscillations (Fig. 25) in accordance with Eq. (7.8) gave $v_F = (1.3 \pm 0.1)\times10^8$ cm/sec for silver at $P = 0$.

Two small effects were observed under pressure: a reduction in the amplitude values of $N_T(\omega)$ because of a reduction in $\Delta_S(\omega)$ and an increase in the oscillation period because of an increase in the ratio v_F/d_N.

The first effect is in full agreement with the theoretical predictions. In fact, the use of the functions $\Delta(\omega)$ found at finite pressures for lead (Fig. 12) shows that if $P = 8$ kbar, then the ratio of the first two maxima of $\sigma(U)/\sigma_0$ for $d_N = 4100$ Å should decrease by a factor of 1.0037 compared with the $P = 0$ case. The experimental value is 1.0032 ± 0.0004.

An increase in the period shows that in the case of silver we have $d[\ln Z_N(0)]/dP \approx 1\times10^{-6}\,\text{bar}^{-1}$, i.e., this value is several times less than for lead, which is a metal with a strong EPI.

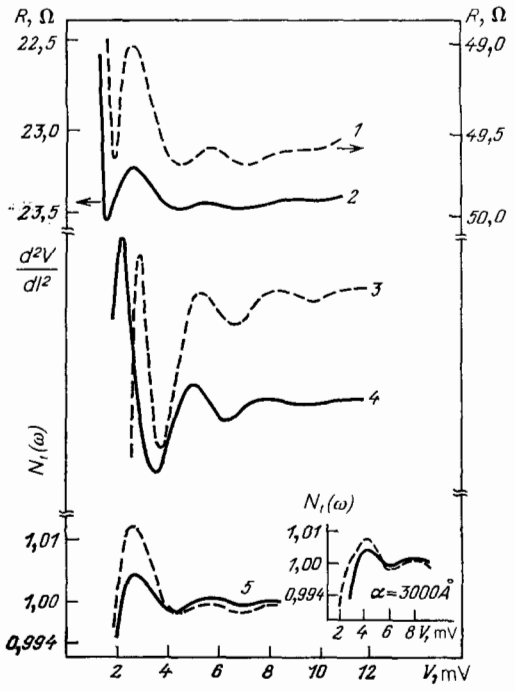

FIG. 25. Influence of pressure on the Andreev-Rowell-McMillan effect.[131] Tunnel characteristics of Al–I–Ag(Pb) junctions with $d_{Ag} = 4100$ Å: 1), 2) dependences of dU/dI on U; 3), 4) dependences of d^2U/dI^2 on U (the continuous curves correspond to $P = 8$ kbar and the dashed curves to $P = 0$); 5) tunnel density of states at zero pressure (the continuous curve is calculated and the dashed curve is experimental). The inset shows the theoretical and experimental densities of states of a contact with $d_{Ag} = 3000$ Å; $T = 1.4$ K.

Experimental observations of standing electron waves in metal plates at high pressures makes it possible to consider the behavior of tunnel oscillations associated with Lifshitz phase transitions when the Fermi surface topology changes.[110] We shall consider the Andreev-Tomasch effect in the case when the Fermi surface acquires a new sheet at some pressure. Since the tunneling of electrons is highly directional, such effects can be observed only in a superconducting film textured along the direction of $\mathbf{p}_c$. If $\varepsilon_c > \varepsilon_F$, then a film of finite thickness exhibits quantum interference between degenerate electron states with the momenta p_+ and p_- and the tunnel conductivity has one oscillatory correction. If $\varepsilon_c < \varepsilon_F$, the situation becomes much more complex because of pairwise interference: a) p_+ and q_+; p_- and q_-; b) q_+ and q_-; c) p_+ and p_-. Three groups of oscillations then appear in the tunnel conductivity.[132]

The ability to observe "topological" effects is not limited to superconductors. A similar oscillatory correction appears in the conductivity of a normal film (Andreev-Rowell-McMillan effect) at voltages above the critical value, when the filling of an energy band just begins.[131]

Finally, we must stress that the quantum size effect is observed also in lead films containing up to 5 at. % of bismuth and thallium.[121,122] This makes it possible to use the quantum size effect in studies of alloys whose energy band structure is relatively little known.

8. CONCLUSIONS

The results obtained show that tunnel spectroscopy is fully compatible with the technique of high pressures and that it opens up new applications of this wide-energy method in studies of solids under pressure. It is now clear that the EPI spectroscopy can be extended also to nonsuperconducting materials.[27,133,134,135] Changes in the magnon, phonon, and molecular spectra of barrier substances can be deduced from experiments on inelastic tunneling.[2,34] Moreover, studies of semimetal-semiconductor phase transitions under pressure are likely to give promising results.[139,140]

It would be very attractive to master the range of even high pressures: exceeding 30–100 kbar. Here, tunnel spectroscopy can contribute to our understanding of the mechanisms of high-pressure superconducting phases and of polymorphic transitions. The effects of intra-atomic transitions and of electron-electron interaction on properties of transition metals, their alloys, and compounds are of interest. However, the technical difficulties are still very great. Promising results have been obtained on Schottky barriers compressed between Bridgman anvils, but it has not been possible to exceed the limit of 12 kbar (Ref. 136). Clearly, tunnel investigations can be carried out in diamond-spacer-diamond hydrostatic microchambers.[137,138] Naturally, at very high pressures one would need new barrier materials and possibly new methods for the formation of barriers, for example, directly under pressure. Certain difficulties can be expected in this direction, but one would hope they will be overcome.

The authors will always remember with gratitude Academician of the Ukrainian Academy of Sciences A. A. Galkin, who actively supported tunnel effect investigations. The authors are also grateful to Prof. N. B. Brandt for his constant and valuable discussions of the topics considered in the present review.

[1)]The results of all this Soviet work at $P = 2$–5 kbar were reported at the Fourteenth All-Union Conference on the Physics and Technology of High Pressures held in Kharkov in June 1967.
[2)]The influence of interfaces on the tunnel current was discussed in Ref. 32.
[3)]The S$_1$IS aluminum films had in this case a high transition temperature of ~ 2 K and the characteristics were recorded at $T \approx 1.2$ K; the NIS aluminum films were in the normal state (here, S is the investigated superconducting metal or alloy).

[1]L. Solymar, *Superconductive Tunneling and Applications*, Chapman and Hall, London, 1972 (Russ. transl., Mir, M., 1974).
[2]E. L. Wolf, *Principles of Electron Tunneling Spectroscopy*, Oxford University Press, 1985.
[3]V. M. Svistunov and M. A. Belogolovskiĭ, Tunnel Spectroscopy of Quasiparticle Excitations in Metals (in Russian), Naukova Dumka, Kiev, 1986.
[4]J. Bardeen, Science **181**, 1209 (1973).
[5]I. Giaever, Phys. Rev. Lett. **5**, 147 (1960); Science **183**, 1253 (1974).
[6]D. H. Douglass Jr. and L. M. Falicov, Prog. Low Temp. Phys. **4**, 97 (1964) (Russ. transl., Nauka, M., 1967, p. 9).
[7]B. T. Geĭlikman, Research on Low Temperature Physics (in Russian), Atomizdat, M., 1979.
[8]W. L. McMillan, Phys. Rev. **167**, 331 (1968).
[9]N. B. Brandt and N. I. Ginzburg, Usp. Fiz. Nauk **98**, 95 (1969) [Sov. Fiz. Usp. **12**, 344 (1969)].
[10]A. A. Galkin and V. M. Svistunov, Phys. Status Solidi **26**, K55 (1968).
[11]N. V. Zavaritskiĭ, E. S. Itskevich, and A. N. Voronovskiĭ, Pis'ma Zh. Eksp. Teor. Fiz. **7**, 271 (1968) [JETP Lett. **7**, 211 (1968)].
[12]J. P. Franck and W. J. Keeler, Phys. Lett. A **25**, 624 (1967).
[13]J. P. Fanck and W. J. Keeler, Phys. Rev. Lett. **20**, 379 (1968).
[14]A. A. Galkin, A. P. Dikii, and V. M. Svistunov, Phys. Status Solidi **30**, K107 (1968).
[15]A. A. Galkin, V. M. Svistunov, and A. P. Dikii, Phys. Status Solidi **35**, 421 (1969).
[16]H. H. Hansen, R. L. Pompi, and T. M. Wu, Phys. Rev. B **8**, 1042 (1973).
[17]P. Nedellec, L. Dumoulin, and R. J. Noer, J. Phys. F **4**, L145 (1974).

[18]P. Nedellec and R. J. Noer, Solid State Commun. **13**, 89 (1973).
[19]P. Guetin and G. Schreder, Phys. Rev. B **5**, 3979 (1972).
[20]H. Wühl, A. Eichler, and J. Witting, Phys. Rev. Lett. **31**, 1393 (1973).
[21]P. N. Trofimenkoff and J. P. Carbotte, Phys. Rev. B **1**, 1136 (1970).
[22]J. P. Carbotte and P. Vashishta, Can. J. Phys. **49**, 1493 (1971).
[23]J. M. Coombes and J. P. Carbotte, Solid State Commun. **54**, 871 (1985).
[24]A. A. Galkin, A. I. D'yachenko, and V. M. Svistunov, Zh. Eksp. Teor. Fiz. **66**, 2262 (1974) [Sov. Phys. JETP **39**, 1115 (1974)].
[25]V. M. Svistunov, A. I. D'yachenko, and M. A. Belogolovskiĭ, J. Low Temp. Phys. **31**, 339 (1978); Fiz. Tverd. Tela (Leningrad) **19**, 2594 (1977) [Sov. Phys. Solid State **19**, 1519 (1977)].
[26]A. I. D'yachenko, Preprint No. 17, Physicotechnical Institute, Academy of Sciences of the Ukrainian SSR, Donetsk, 1981.
[27]V. M. Svistunov, M. A. Belogolovskiĭ, O. I. Chernyak, A. I. Khachaturov, and A. P. Kvachev, Zh. Eksp. Teor. Fiz. **84**, 1781 (1983) [Sov. Phys. JETP **57**, 1038 (1983)].
[28]A. P. Kvachev, V. M. Svistunov, and V. A. Chubar', Fiz. Tekh. Vys. Davlenii No. 4, 70 (1981).
[29]A. P. Kvachev and V. M. Svistunov, Author's Certificate No. 834 608 [in Russian], appl. April 17, 1978; publ. May 30, 1981.
[30]A. Barone and G. Paterno, *Physics and Applications of the Josephson Effect*, Wiley, New York, 1982 (Russ. transl., Mir, M., 1984).
[31]I. P. Revokatova and A. P. Silin, Usp. Fiz. Nauk **142**, 159 (1984) [Sov. Phys. Usp **27**, 76 (1984)].
[32]M. V. Krylov and R. A. Suris, Zh. Eksp. Teor. Fiz. **88**, 2204 (1985) [Sov. Phys. JETP **61**, 1303 (1985)].
[33]W. F. Brinkman, R. C. Dynes, and J. M. Rowell, J. Appl. Phys. **41**, 1915 (1970).
[34]P. K. Hansma (ed.), *Tunneling Spectroscopy: Capabilities, Applications, and new Techniques*, Plenum Press, New York, 1982.
[35]J. R. Schrieffer, in: *Tunneling Phenomena in Solids* (Lectures presented at the 1967 NATO Advanced Study Institute at Risö, Denmark, ed. by E. Burstein and S. Lundqvist), Plenum Press, New York, 1969, p. 287 (Russ. transl., Mir, M., 1973, p. 274).
[36]V. L. Ginzburg and D. A. Kirzhnits (eds.), Problem of High-Temperature Superconductivity (in Russian), Nauka, M., 1977, Chap. 4.
[37]D. J. Scalapino and P. W. Anderson, Phys. Rev. **133**, A921 (1964).
[38]Yu. F. Revenko, A. I. D'yachenko, V. M. Svistunov, and B. Schoneich, Fiz. Nizk. Temp. **6**, 1304 (1980) [Sov. J. Low Temp. Phys. **6**, 635 (1980)].
[39]S. I. Vedeneev, Thermodynamics and Electrodynamics of Superconductors (in Russian), Nauka, M., 1983, p. 47.
[40]W. L. McMillan, Phys. Rev. **175**, 537 (1968).
[41]V. M. Svistunov and M. A. Belogolovskiĭ, Fiz. Nizk. Temp. **3**, 869 (1977)([Sov. J. Low Temp. Phys. **3**, 421 (1977)].
[42]P. G. De Gennes and D. Saint-James, Phys. Lett. **4**, 151 (1963).
[43]E. L. Wolf and G. B. Arnold, Phys. Rep. **91**, 31 (1982).
[44]E. L. Wolf, J. Zasadzinski J. W. Osmun, and G. B. Arnold, Solid State Commun. **31**, 321 (1979).
[45]B. Mitrović and J. P. Carbotte, Physica B + C (Utrecht) **108**, 977 (1981).
[46]H. G. Zarate and J. P. Carbotte, J. Low Temp. Phys. **57**, 291 (1984).
[47]W. L. McMillan and J. M. Rowell, in: *Superconductivity* (ed. by R. D. Parks), Vol 1, Dekker, New York, 1969, p. 561.
[48]N. B. Brandt, E. S. Itskevich, and N. Ya. Minina, Usp. Fiz. Nauk **104**, 459 (1971) [Sov. Phys. Usp. **14**, 438 (1972)].
[49]E. S. Itskevich, Prib. Tekh. Eksp. No. 4, 148 (1963).
[50]B. G. Lazarev and L. Kan, Zh. Eksp. Teor. Fiz. **14**, 439 (1944).
[51]C. C. Bradley, *High Pressure Methods in Solid State Research*, Butterworths, London; Plenum Press, New York, 1968 (Russ. transl., Mir, M., 1972).
[52]V. M. Svistunov, O.I. Chernyak, M. A. Belogolovskiĭ, and A. I. D'yachenko, Fiz. Tekh. Vys. Davleniĭ No. 1, 75 (1980).
[53]V. M. Svistunov, O. I. Chernyak, M. A. Belogolovskiĭ, and A. I. D'yachenko, Philos. Mag. B **43**, 75 (1981).
[54]W. L. Feldmann and J. M. Rowell, J. Appl. Phys. **40**, 312 (1969).
[55]J. S. Rogers, Rev. Sci. Instrum. **41**, 1184 (1970).
[56]B. L. Blackford, Rev. Sci. Instrum. **42**, 1198 (1971).
[57]M. V. Moody, J. L. Paterson, and R. L. Ciali, Rev. Sci. Instrum. **50**, 903 (1979).
[58]Th. L. Paoli and J. F. Svacek, Rev. Sci. Instrum. **47**, 1016 (1976).
[59]J. G. Adler and J. Straus, Rev. Sci. Instrum. **46**, 158 (1975).
[60]A. G. Dargis, Rev. Sci. Instrum. **52**, 46 (1981).
[61]V. M. Svistunov and O. I. Chernyak, Fiz. Tekh. Vys. Davleniĭ No. 10, 26 (1982).
[62]M. A. Belogolovskiĭ, A. I. D'yachenko, and A. I. Khachaturov, Ukr. Fiz. Zh. **27**, 628 (1982).
[63]H. Wehr and K. Knorr, Z. Phys. B **33**, 21 (1979).
[64]C. A. Mead, in: *Tunneling Phenomena in Solids* (Lectures presented at the 1967 NATO advanced Study Institute at Risö, Denmark, ed. by E. Burstein and S. Lundqvist, Plenum Press, New York, 1969, p. 127 (Russ. transl., Mir, M., 1973, p. 125).
[65]S. L. Kurtin, T. C. McGill, and C. A. Mead, Phys. Rev. B **3**, 3368 (1971).
[66]C. A. Swenson, Solid State Phys. **11**, 41 (1960) [Russ. transl., IL, M., 1963).
[67]M. A. Belogolovskiĭ, A. A. Galkin, and V. M. Svistunov, Fiz. Tverd. Tela (Leningrad) **17**, 145 (1975) [Sov. Phys. Solid State **17**, 83 (1975)].
[68]A. E. Gorbonosov and I.O. Kulik, Zh. Eksp. Teor. Fiz. **55**, 876 (1968) [Sov. Phys. JETP **28**, 455 (1969).
[69]A. A. Galkin, V. M. Svistunov, A. P. Dikiĭ, and V. N. Taranenko, Zh. Eksp. Teor. Fiz. **59**, 77 (1970) [Sov. Phys. JETP **32**, 44 (1971)].
[70]B. L. Blackford and R. H. March, Phys. Rev. **186**, 397 (1969).
[71]A. A. Galkin, M. A. Belogolovskiĭ, and V. M. Svistunov, Dopov, Akad. Nauk Ukr. RSR Ser. A Fiz.-Mat. Tekh. Nauki No. 11, 1019 (1975).
[72]C. R. Leavens and J. P. Carbotte, Can. J. Phys. **50**, 2568 (1972).
[73]A. A. Galkin, V. M. Svistunov, O. I. Chernyak (Chernjak), and M. A. Belogolovskiĭ, Solid State Commun. **13**, 1095 (1973).
[74]A. A. Galkin, V. M. Svistunov, Yu. F. Revenko, and V. M. Mostovoĭ, Fiz. Tverd. Tela (Leningrad) **18**, 1986 (1976) [Sov. Phys. Solid State **18**, 1156 (1976)].
[75]Yu. F. Revenko, V. M. Mostovoĭ, and V. M. Svistunov, Fiz. Nizk. Temp. 7, 141 (1981) [Sov. J. Low Temp. Phys. **7**, 69 (1981)]; V. M. Mostovoĭ, Yu. F. Revenko, and V. M. Svistunov, Zh. Eksp. Teor. Fiz. **80**, 235 (1981) [Sov. Phys. JETP **53**, 119 (1981)].
[76]V. M. Svistunov, A. P. Dikiĭ, and A. I. D'yachenko, Fiz. Nizk. Temp. **5**, 711 (1979) [Sov. J. Low Temp. Phys. **5**, 337 (1979)].
[77]N. V. Zavaritskiĭ, E. S. Itskevich, and A. N. Voronovskiĭ, Zh. Eksp. Teor. Fiz. **60**, 1408 (1971) [Sov. Phys. JETP **33**, 762 (1971)].
[78]P. W. Wright and J. P. Franck, J. Low Temp. Phys. **27**, 459 (1977).
[79]V. M. Svistunov and Yu. F. Revenko, Zh. Eksp. Teor. Fiz. **73**, 1803 (1977) [Sov. Phys. JETP **46**, 947 (1977)].
[80]A. A. Galkin, V. M. Svistunov, O. I. Chernyak, and M. A. Belogolovskiĭ, Dokl. Akad. Nauk SSSR **210**, 815 (1973) [Sov. Phys. Dokl. **18**, 411 (1973)].
[81]K. Shimada, Phys. Status Solidi B **61**, 701 (1974).
[82]N. V. Zavaritskiĭ, Usp. Fiz. Nauk **108**, 241 (1972) [Sov. Phys. Usp. **15**, 608 (1973)].
[83]V. M. Svistunov, A. I. D'yachenko, and O. I. Chernyak, Fiz. Tverd. Tela (Leningrad) **19**, 1994 (1977) [Sov. Phys. Solid State **19**, 1167 (1977)].
[84]B. I. Borodaĭ and V. M. Svistunov, Fiz. Nizk. Temp. **6**, 308 (1980) [Sov. J. Low Temp. Phys. **6**, 146 (1980)].
[85]V. M. Svistunov, M. A. Belogolovskiĭ, Yu. F. Revenko, and O. I. Chernyak, Vestn. Akad. Nauk Ukr. RSR No. 2, 8 (1984).
[86]V. M. Mostovoĭ and Yu. F. Revenko, Fiz. Nizk.Temp. **7**, 658 (1981) [Sov. J. Low Temp. Phys. **7**, 324 (1981)].
[87]P. Nedellec, Thèse, Orsay, France, 1975.
[88]P. Ochik. V. M. Svistunov, M. A. Belogolovskiĭ, and A. I. D'yachenko, Fiz. Tverd. Tela (Leningrad) **20**, 1903 (1978) [Sov. Phys. Solid State **20**, 1101 (1978)]; A. I. D'yachenko, Fiz. Nizk. Temp. **5**, 440 (1979) [Sov. J. Low Temp. Phys. **5**, 210 (1979)].
[89]P. K. Lam and M. L. Cohen, Phys. Lett. A **97**, 114 (1983).
[90]K. A. Gschneidner Jr., Solid State Phys. **16**, 275 (1964).
[91]D. L. Waldorf and G. A. Alers, J. Appl. Phys. **33**, 3266 (1962).
[92]S. Alterovitz and D. E. Mapother, Phys. Rev. B **11**, 139 (1975).
[93]N. B. Brandt, I. V. Berman, and Yu. P. Kurkin, Zh. Eksp. Teor. Fiz. **69**, 1710 (1975) [Sov. Phys. JETP **42**, 869 (1975)].
[94]J. Bostock, V. Diadiuk, W. N. Cheung, K. H. Lo, R. M. Rose, and M. L. A. MacVicar, Phys. Rev. Lett. **36**, 603 (1976).
[95]R. Glocker and L. Fritsche, Phys. Status Solidi B **88**, 649 (1978).
[96]P. B. Allen and R. C. Dynes, Phys. Rev. B **12**, 905 (1975).
[97]C. R. Leavens, A. H. MacDodnald, and R. Taylor, Phys. Rev. B **27**, 1352 (1983).
[98]S. V. Vonsovskiĭ, Yu. A. Izyumov, and É. Z. Kurmaev, Superconductivity of Transition Metals, Their Alloys, and Compounds (in Russian), Nauka, M., 1977.
[99]K. I. Wysokinski and A. L. Kuzemsky, J. Low Temp. Phys. **52**, 81 (1983).
[100]V. V. Nemoshkalenko, A. V. Zhalko-Titarenko, V. N. Antonov, Vl. N. Antonov, and E. Mrosan, Phys. Status Solidi B **106**, K117 (1981).
[101]J. C. Swihart, D. G. Garrett, and B. K. Bhattacharyya, Phys. Lett. A **85**, 295 (1981).
[102]L. V. Meisel and P. J. Cote, Phys. Rev. B **23**, 5834 (1981).
[103]M. Hansen and K. Anderko, *Constitution of Binary Alloys*, 2nd ed., McGraw-Hill, New York, 1958 (Russ. transl., Metallurgizdat, M., 1962).
[104]B. I. Borodaĭ and V. M. Svistunov, Fiz. Tverd. Tela (Leningrad) **20**, 1013 (1978) [Sov. Phys. Solid State **20**, 585 (1978)].
[105]B. I. Borodaĭ and V. M. Svistunov, Fiz. Tverd. Tela (Leningrad) **23**,

130 (1981) [Sov. Phys. Solid State **23**,73 (1981)].
[106]I. L. Aptekar' and V. B. Baskakova, Dokl. Akad. Nauk SSSR **191**, 1305 (1970).
[107]V. M. Svistunov, M. A. Belogolovskiĭ, V. Yu. Tarenkov, and O. I. Chernyak, Zh. Eksp. Teor. Fiz. **76**, 630 (1979) [Sov. Phys. JETP **49**, 315 (1979)].
[108]D. E. Gordon and B. C. Deaton, Phys. Rev. B **6**, 2982 (1972).
[109]L. Dagens, J. Phys. F **8**, 2093 (1978).
[110]I. M. Lifshitz, Zh. Eksp. Teor. Fiz. **38**, 1569 (1960) [Sov. Phys. JETP **11**, 1130 (1960)].
[111]B. G. Lazarev, L. S. Lazareva, V. I. Makarov, and T. A. Ignat'eva, Zh. Eksp. Teor. Fiz. **48**, 1065 (1965) [Sov. Phys. JETP **21**, 711 (1965)].
[112]V. I. Makarov and V. G. Bar'yakhtar, Zh. Eksp. Teor. Fiz. **48**, 1717 (1965) [Sov. Phys. JETP **21**, 1151 (1965)].
[113]I. Ya. Volynskiĭ, V. I. Makarov, and V. V. Gann, Zh. Eksp. Teor. Fiz. **69**, 1019 [Sov. Phys. JETP **42**, 518 (1975].
[114]A. A. Galkin, V. M. Svistunov, Yu. F. Revenko, V. M. Mostovoĭ, and M. A. Belogolovskiĭ, Pis'ma Zh. Eksp. Teor. Fiz. **23**, 189 (1976) [JETP Lett. **23**, 167 (1976)].
[115]V. M. Svistunov, A. I. D'yachenko, and M. A. Belogolovskiĭ, Fiz. Tverd. Tela (Leningrad **18**, 3217 (1976) [Sov. Phys. Solid State **18**, 1877 (1976)].
[116]V. I. Makarov, Zh. Eksp. Teor. Fiz. **78**, 1852 (1980) [Sov. Phys. JETP **51**, 930 (1980)]; Fiz. Nizk. Temp. **8**, 608 (1982) [Sov. J. Low Temp. Phys. **8**, 302 (1982)].
[117]L. Dagens, J. Phys. (Paris) Lett. **37**, L-37 (1976).
[118]I. M. Lifshitz and A. M. Kosevich, Dokl. Akad. Nauk SSSR **91**, 795 (1953).
[119]G. A. Gogadze and I. O. Kulik, Fiz. Tverd. Tela (Leningrad) **7**, 432 (1965) [Sov. Phys. Solid State 7, 345 (1965)].
[120]V. N. Lutskiĭ, D. N. Korneev, and M. I. Elinson, Pis'ma Zh. Eksp. Teor. Fiz. **4**, 267 (1966) [JETP Lett. **4**, 179 (1966)].
[121]R. C. Jaklevic and J. Lambe, Phys. Rev. B **12**, 4146 (19 5).
[122]A. A. Galkin, V. M. Svistunov, A. I. D'yachenko, and V. Yu. Tarenkov, Pis'ma Zh. Eksp. Teor. Fiz. **21**, 259 (1975) [JETP Lett. **21**, 118 (1975)].
[123]A. A. Galkin, V. M. Svistunov, A. I. D'yachenko, and V. Yu. Tarenkov, Proc. Fourteenth Intern. Conf. on Low Temperature Physics, Otaniemi, Finland, 1975, Part III, publ. by North-Holland, Amsterdam, 1975, p. 498.
[124]V. M. Svistunov, V. Yu. Tarenkov, and V. T. Vitchinkin, Fiz. Tverd. Tela (Leningrad) **21**, 3340 (1979) [Sov. Phys. Solid State **21**, 1929 (1979)].
[125]Yu. F. Komnik, Physics of Metal Films (in Russian), Atomizdat, M., 1979.
[126]D. A. Papaconstantopoulos, A. D. Zdetsis, and E. N. Economou, Solid State Commun. **27**, 1189 (1978).
[127]M. A. Belogolovskiĭ, A. A. Galkin, and V. M. Svistunov, Zh. Eksp. Teor. Fiz. **69**, 1795 (1975) [Sov. Phys. JETP **42**, 912 (1975)].
[128]A. F.Andreev, Zh. Eksp. Teor. Fiz. **46**, 1823 (1964) [Sov. Phys. JETP **19**, 1228 (1964)].
[129]W. A.Tomasch, in: *Tunneling Phenomena in Solids* (Lectures presented at the 1967 NATO Advanced Study Institute at Risö, Denmrk, ed. by E. Burstein and S. Lundqvist), Plenum Press, New York, 1969, p. 315 (Russ. transl., Mir, M., 1973, p. 300).
[130]V. M. Svistunov and V. Yu. Tarenkov, Pis'ma Zh. Eksp. Teor. Fiz. **26**, 34 (1977) [JETP Lett. **26**, 30 (1977)].
[131]V. M. Svistunov, M. A. Belogolovskiĭ, V. Yu. Tarenkov, and N. D. Tsapko, Fiz. Tverd. Tela (Leningrad) **22**, 919 (1980) [Sov. Phys. Solid State **22**, 539 (1980)].
[132]V. M. Svistunov and M. A. Belogolovskiĭ, Phys. Lett. A **67**, 419 (1976).
[133]O. I. Chernyak, A. I. Khachaturov, and A. P. Kvachev, J. Phys. F **14**, 2359 (1984).
[134]C. R. Leavens, Solid State Commun. **55**, 13 (1985).
[135]V. M. Svistunov and M. A. Belogolovskiĭ, Vestn. Akad. Nauk Ukr. RSR No. 2, 25 (1986); Fiz. Tverd. Tela (Leningrad) **28**, 284 (1986) [Sov. Phys. Solid State **28**, 156 (1986)].
[136]V. M. Svistunov and N. D. Tsapko, Fiz. Tekh. Vys. Davleniĭ No. 16, 13 (1984).
[137]S. M. Stishov, Usp. Fiz. Nauk **127**, 719 (1979) [Sov. Phys. Usp. **22**, 283 (1979)].
[138]A. Jayaraman, Rev. Mod. Phys. **55**, 65 (1983).
[139]J. P. Sorbier and M. Gasgnier, J. Phys. F **10**, 2279 (1980).
[140]M. C. Zatet, L. Gunther, B. A. Ratnam, and P. M. Tedrow, J. Appl. Phys. **59**, 191 (1986).

Translated by A. Tybulewicz